remote sensing

Article

Masi Entropy for Satellite Color Image Segmentation Using Tournament-Based Lévy Multiverse Optimization Algorithm

Heming Jia [1], Xiaoxu Peng [1], Wenlong Song [1,*], Diego Oliva [2], Chunbo Lang [1] and Yao Li [1]

[1] College of Mechanical and Electrical Engineering, Northeast Forestry University, Harbin 150040, China; jiaheming@nefu.edu.cn (H.J.); pengxiaoxu@nefu.edu.cn (X.P.); langchunbo@nefu.edu.cn (C.L.); liyao@nefu.edu.cn (Y.L.)

[2] Departamento de Ciencias Computacionales, Universidad de Guadalajara, CUCEI, Av. Revolución 1500, 44430 Guadalajara, Jalisco, Mexico; diego.oliva@cucei.udg.mx

* Correspondence: swl@nefu.edu.cn

Received: 3 April 2019; Accepted: 16 April 2019; Published: 18 April 2019

Abstract: A novel multilevel threshold segmentation method for color satellite images based on Masi entropy is proposed in this paper. Lévy multiverse optimization algorithm (LMVO) has a strong advantage over the traditional multiverse optimization algorithm (MVO) in finding the optimal solution for the segmentation in the three channels of an RGB image. As the work advancement introduces a Lévy multiverse optimization algorithm which uses tournament selection instead of roulette wheel selection, and updates some formulas in the algorithm with mutation factor. Then, the proposal is called TLMVO, and another advantage is that the population diversity of the algorithm in the latest iterations is maintained. The Masi entropy is used as an application and combined with the improved TLMVO algorithm for satellite color image segmentation. Masi entropy combines the additivity of Renyi entropy and the non-extensibility of Tsallis entropy. By increasing the number of thesholds, the quality of segmenttion becomes better, then the dimensionality of the problem also increases. Fitness function value, average CPU running time, Peak Signal-to-Noise Ratio (PSNR), Structural Similarity Index (SSIM) and Feature Similarity Index (FSIM) were used to evaluate the segmentation results. Further statistical evaluation was given by Wilcoxon's rank sum test and Friedman test. The experimental results show that the TLMVO algorithm has wide adaptability to high-dimensional optimization problems, and has obvious advantages in objective function value, image quality detection, convergence performance and robustness.

Keywords: multilevel threshold segmentation; Masi entropy; multiverse optimization algorithm; Lévy multiverse optimization algorithm; tournament selection

1. Introduction

With the booming of artificial intelligence (IA) technology, in order to meet people's needs, the practicality of computer vision technology is highly emphasized. Image segmentation is one of the main problems of digital image processing technology and machine vision technology [1], which can be either gray image segmentation or color image segmentation. By comparison, grayscale images contain less information. Meanwhile, color images contain more color information such as hue and saturation [2,3]. On the other hand, images have a wide range of applications in the fields of geographic graphic information systems, astronomy and earth science research. It is necessary to locate objects and boundaries accurately in satellite images. Therefore, color satellite image segmentation is a critical and challenging topic [4–6].

The existing image segmentation methods are mainly divided into the following categories: threshold segmentation, region growth, region division and merging, watershed algorithm, edge detection, histogram method, cluster analysis and wavelet transform among others. Threshold segmentation is widely used and it can be divided into bi-level threshold and multilevel threshold [7,8]. Bi-level threshold is the simplest segmentation method, as long as one gray value can be determined to divide the image into two regions of interest (ROI) [9]. In actual image processing, color images contain more than two ROI, for that reason only multilevel threshold methods can be adopted. The pixels are divided into groups, and, within each group, the pixels have intensity values within a specific range. Sezgin et al. [10] divided the image thresholding techniques into six groups according to information. These groups include methods based on histogram, clustering, entropy, object attributes, spatial and local information. The segmentation techniques that employ histograms and statistical information (variance of entropy) are the most used due to its practicality. An example of these kinds of approaches is Otsu's algorithm, where each bar of the histogram represents a gray scale. In Otsu, the best threshold is obtained by computing the between class variance that exists among the two classes [11]. The higher the between-class variance is, the better the segmentation effect will be. As a basic and effective segmentation method, Otsu has been highly regarded and widely used for a long time. Today, people still have not stopped researching and utilizing it. In 2019, an accurate, scalable, polynomial time multistage threshold segmentation algorithm based on Otsu method has just been proposed [12]. Entropy-based methods, with their virtue of the charming basic mathematical concepts of entropy, has been infinitely improved and updated by researchers. In the image, the uniform region corresponds to the minimum entropy, while the non-uniform region defines the maximum entropy. Therefore, a better segmentation effect can be obtained by obtaining a larger Boltzmann–Gibbs entropy of the segmented image [13,14]. Therefore, entropy-based algorithms with different characteristics are well known. For instance, Fuzzy entropy [15], Renyi entropy [16], Shannon entropy [17], Tsallis entropy [18], and Kapur entropy [19]. Entropy-based thresholding has been widely used in multilevel image segmentation.

The main drawback of segmentation using entropy is to find the best configuration of thresholds. Each threshold increases the computational effort—for that reason, it is required the use of a search algorithm. Considering the above, segmentation is considered as an optimization problem in the literature, where entropy is used as an objective function. An interesting approach that employs optimization considers a hybridization of genetic algorithms and cross entropy methods (GACE) were proposed for solving continuous optimization [20]. An improved fuzzy entropy and Lévy flying firefly algorithm (FA) method is used for color image threshold segmentation [21]. By maximizing Shannon entropy or fuzzy entropy, the FA is utilized to image segmentation [22]. On the other hand, in 2005, Masi et al. proposed a newer and more coordinated Masi entropy which integrates the additivity of Renyi entropy and the non-extensibility of Tsallis entropy [23]. Fundamentally, Masi entropy is also a kind of innovation of Shannon entropy. By adjusting the entropy parameter r of Masi entropy, its application scope can be expanded. Swapnil Shubham et al. applied the concept of Masi entropy to multilevel thresholding of color images, and confirmed its potential to achieve a wide range of objectives in efficient multilevel image segmentation [24,25].

The prosperity of optimization field drives the development of many fields. The cross-fusion of different areas through optimization algorithm can bring more immeasurable value to people. With the introduction of the No Free Lunch (NFL) theorem, people have realized the universality of optimization [26]. In 2002, E. G. Talbi published an article about a taxonomy of hybrid metaheuristics [27]. E. A. Baniani proposed a hybrid particle swarm optimization (PSO) algorithm and a genetic algorithm (GA) in 2013 for multilevel maximum entropy criterion threshold selection [28]. A hybrid whale algorithm and simulated annealing optimization algorithm have been applied to feature selection in 2017 [29]. At present, the combination of optimization algorithm and image segmentation can be said to be very mature, with a relatively complete system. With the introduction of more new and effective algorithms and the improvement of image segmentation methods, the prospects in this field are very promising. An approach called Multiverse Optimization (MVO) was first proposed by S. Mirjalili in 2015, which belongs to the physically inspired metaheuristic algorithms [30]. With the proposal, it has received successive improvements and utilization by scholars. In 2016, MVO was applied to the study of photovoltaic parameters, and five parameters of the single-diode model of photovoltaic cells were extracted [31]. In 2017, MVO mixed the PSO to solve the problem of global numerical optimization and reactive optimization scheduling [32]. In 2018, China's energy consumption was estimated using a self-adaptive MVO optimizer support vector machine with rolling cross-validation [33]. In 2019, the multi-objective MVO algorithm was utilized for grayscale image segmentation [34]. Compared with the traditional algorithm, the MVO algorithm has better performance, but there are still some flaws in slow convergence, low accuracy and ease of being trapped in the local optimal. Roulette wheel selection is used as a mechanism for determining the optimal universe in MVO. However, when the fitness function of the algorithm is so close at the later stage, the selection advantage of the optimal universe is greatly weakened, and it is easy to fall into local solutions. To solve these drawbacks, this paper proposed the use of the tournament selection. By calculating the reciprocal of fitness function, the optimal universe can be determined. This is because, in the minimization problem, tournament selection is better than roulette wheel selection, and can maintain a strong and continuous update even at the end of the iterative process, which has been proved in the related literature [35,36].

Regarding the improvement of MVO, an enhanced version that merges the MVO with Lévy flight (LMVO) has recently been proposed [37]. When Lévy random walk is added to MVO appropriately, the algorithm not only improves the accuracy, but also enhances the robustness. As a promotion of the work, the mutation factor is added to the location update while replacing the screening mechanism, which ensures the diversity of the population in the later stage of the algorithm. These improvements are conducive to achieving a better balance between the exploration and exploitation of the algorithm, improving the accuracy of local optimization and the ability of global optimization. Therefore, this article presents an improved version of the LMVO called TLMVO including a tournament selection operator instead of the roulette wheel. As a real application, the TLMVO has been used for image thresholding using the Masi entropy as a fitness function. The proposal is tested using color satellite images that are more complicated than benchmark datasets. The performance of the improved algorithm is evaluated by considering the accuracy of the optimization, the quality of the segmentation and a statistical comparative analysis.

The remainder of this paper is organized as follows: Section 2 outlines the multi-threshold problem and Masi entropy. Section 3 gives an overview of MVO followed by its mathematical model. The proposed TLMVO-based multilevel thresholding method is presented in Section 4, where the basic instructions of three strategy are also illustrated. Simulation experiments and results analysis are described in Section 5. Finally, Section 6 concludes the work and suggests some directions for future studies.

2. Problem Statement

2.1. Summary Description of Multilevel Thresholding

Assuming that a color image with dimension $M \times N$ has L gray values $[0, 1, \ldots, L-1]$ for each of the color frame (red, green, and blue). L is considered as 256.

In each frame, let n_i represent the number of pixels with gray value of i. Correspondingly, the distribution probability p_i of the i-th gray value is indicated as:

$$p_i = \frac{n_i}{M \times N}, \tag{1}$$

$$\sum_{0}^{L-1} p_i = 1, p_i \geq 0. \tag{2}$$

Suppose there are K thresholds. Then, $t_1, t_2, \cdots, t_K$ can divide the the gray levels of the given image into $K+1$ classes, for which t represents threshold value. For multilevel thresholding, define different classes as:

$$\begin{aligned} &[0, t_1 - 1] \in M_0 \\ &[t_1, t_2 - 1] \in M_1 \\ &\cdots\cdots \\ &[t_K, L - 1] \in M_K, \end{aligned} \tag{3}$$

where $t_1 < t_2 < \ldots < t_K$. Then $t_0 = 0$ and $t_{K+1} = L$.

2.2. Masi Entropy

Most of the entropy testing methods for image segmentation need to obtain the maximum entropy. The effect of the segmentation between the object and the background depends on the value of the entropy. Experimental results have shown that fitness function value of Kapur's, Tsallis, Renyi's, and Masi's entropy are sorted as Kapur's < Tsallis < Renyi's < Masi's [24].

For multilevel thresholding image segmentation of K thresholds, the class probabilities are defined as:

$$\omega_0 = \sum_{i=0}^{t_1-1} p_i, \omega_1 = \sum_{i=t_1}^{t_2-1} p_i, \omega_2 = \sum_{i=t_2}^{t_3-1} p_i, \ldots, \omega_K = \sum_{i=t_K}^{L-1} p_i. \tag{4}$$

Furthermore, the probability distribution defined above is normalized, and each new set of probability distribution is obtained in different classes, which can be expressed by mathematical formulas as:

$$DM_0 : \frac{p_0}{\omega_0}, \frac{p_1}{\omega_0}, \ldots, \frac{p_{t_1-1}}{\omega_0}, DM_1 : \frac{p_{t_1}}{\omega_1}, \frac{p_{t_1+1}}{\omega_1}, \ldots, \frac{p_{t_2-1}}{\omega_1}, DM_K : \frac{p_{t_K}}{\omega_K}, \frac{p_{t_K+1}}{\omega_K}, \ldots, \frac{p_{L-1}}{\omega_K}. \tag{5}$$

The entropy value of the image can be represented as:

$$H_j = \frac{1}{1-r} \log\left[1 - (1-r) \sum_{i=t_j}^{t_{j+1}-1} \left(\frac{p_i}{\omega_j}\right) \log\left(\frac{p_i}{\omega_j}\right)\right], \tag{6}$$

where $0 \le j \le K$. The entropy is represented by H, and r is the value of the entropic parameter which is set to 1.2. Then, the objective function can be mathematically described by:

$$\psi(t_1, t_2, \cdots, t_K) = H_1 + H_2 + \ldots + H_K, \tag{7}$$

for which the definition of the optimal threshold of Masi is as follows:

$$\left\{t_1^*, t_2^*, \cdots, t_K^*\right\} = \underset{0 < t_1 < t_2 \cdots < t_K < L-1}{\arg\max} \left(\psi(t_1, t_2, \cdots, t_K)\right). \tag{8}$$

For color images, as described above, Masi entropy is calculated for each color channel of the image. Using algorithms, the objective function defined in Equation (7) is maximized by Equation (8), the threshold of each channel is calculated separately, and the segmented RGB images are formed by using these thresholds. Using the resulting optimal threshold, a final segmented image is formed.

3. Multiverse Optimization Algorithm

The Basic Multiverse Optimization Algorithm

Inspired by the Big Bang and Quantum Mechanics [38,39], each universe is regarded as a possible solution vector, treating an object in the universe as a variable in the corresponding solution vector. Each universe has a corresponding inflation rate, which is seen as fitness function value. Black holes are used to receive objects and exist in the universe with a low rate of inflation; white holes are used to send out objects and exist in the universe with a high rate of inflation; wormholes are tunnels between black holes and white holes; and the value of the expansion ratio is screened by a roulette mechanism to produce a white hole. According to the above rules, balanced exploration and development achieve optimal universe renewal. The following formulas correspond to the mathematical algorithmic models of the multiverse.

Mathematical Model

Considering the following definition of a universe:

$$U = \begin{bmatrix} x_1^1 & x_1^2 & \cdots & x_1^d \\ x_2^1 & x_2^2 & \cdots & x_2^d \\ \cdots & \cdots & \cdots & \cdots \\ x_n^1 & x_n^2 & \cdots & x_n^d \end{bmatrix}. \tag{9}$$

d represents the number of parameters and n refers to the number of solutions. Each element of U is then defined as:

$$x_i^j = \begin{cases} x_k^j & r_1 < NI\{U_i \\ x_i^j & r_1 \geq NI\{U_i \end{cases}, \tag{10}$$

where x_i^j represents the j-th parameter of i-th universe, U_i represents the i-th universe, $NI(U_i)$ refers to the standard inflation rate of the i-th universe and x_k^j indicates the j-th parameter of k-th universe selected by a roulette wheel selection mechanism.

The new positions of the elements in the optimal universe are obtained by Equation (11):

$$x_{i+1}^j = \begin{cases} \begin{cases} x_i^j + TDR \times \{\{ub_j - lb_j \times r_4 + lb_j & r_3 < H \\ x_i^j - TDR \times \{\{ub_j - lb_j \times r_4 + lb_j & r_3 \geq H \end{cases} & r_2 < WEP \\ x_i^j & r_2 \geq WEP \end{cases}, \tag{11}$$

where $H = 0.5$, r_1, r_2, r_3, r_4 are random numbers in the interval [0,1]. Wormhole existence probability (WEP) is as follows:

$$WEP = \min + l \times \left(\frac{\max - \min}{L}\right). \tag{12}$$

Here, $\min = 0.2$, $\max = 1$, l is the current iteration, and L is the maximum iteration. Travelling distance rate (TDR) is:

$$TDR = 1 - \frac{l^{1/p}}{L^{1/p}}. \tag{13}$$

p denotes the accuracy of mining capability. Both TDR and WEP are coefficients and the relationship between them is shown in Figure 1. Local and global optimization are realized through Equations (10) and (11). The pseudo-code of the MVO algorithm is given in Algorithm 1.

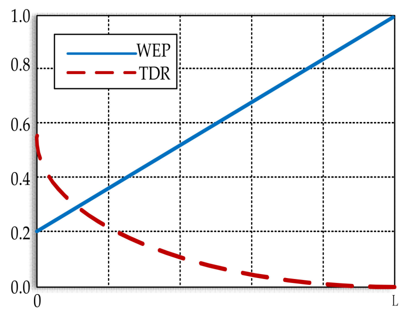

Figure 1. WEP versus TDP [30].

Algorithm 1 Pseudo-Code of the Traditional MVO Algorithm

Initialize the positions of universes;
Randomly initialize the population *Sorted Universes (SU)*;
While *iteration* < *Max_iteration* **do**
For each universe indexed by ***i***
Check if any search agent goes beyond the search space and amend it;
Calculate the objective function value of each universe (Inflation_rates of the universe)(NI);
Update the best solution Best_universe, and WEP and TDR;
For each object indexed by ***j***
Using Roulette Wheel Selection methods and the idea of wormhole, white hole, and black hole to update the universe using *Equation (10)*
Update the position of object in the optimal universe using *Equation (11)*
End for
End for
End while

4. The Proposed Multilevel Thresholding Algorithm

The idea of MVO optimization algorithm is interesting, which combines physical concepts such as multiverse, wormhole, white hole, black hole and so on. The roulette selection mechanism is utilized in the selection of white holes/black holes, which makes the generation of black holes/white holes in the whole universe very random. Location updates are limited by factors such as current location and object range. Based on the above, in this paper, the roulette selection mechanism was replaced with the tournament selection. Inspired by Cuckoo Search Optimization (CS) [40,41], Flower Pollination Algorithm (FPA) [42,43] and Martingale Algorithm (DA) [44], LMVO has introduced the concept of Lévy flight into white hole/black update. Based on this, a better algorithm model is obtained by adding a mutation factor in this paper [37]. Taking the Masi entropy method as the objective function, through the proposed multiverse optimization algorithm, the maximum value of Masi entropy can be found quickly and stably. Finally, the optimal thresholds (t_R, t_G, t_B) of three different color components (red, green and blue) in the input color image are determined, so as to achieve a better image segmentation effect.

4.1. Selection Schemes

In this section, the selection schemes are described. That is, the roulette selection mechanism of the original algorithm and the tournament selection used to replace the roulette selection mechanism in the algorithm proposed in this paper. Both mechanisms are selected based on fitness function values. Selection strategies are to judge the current individual and determine which individual is used for position update according to the fitness value in the hope of obtaining a higher fitness value in the next iteration. The selection strategy is to judge the current individual and determine which individual to use for location update according to the fitness value. Different selection strategies have different calculation methods of selection, and a more suitable selection mechanism with the algorithm can easily obtain better results to a large extent [45].

4.1.1. Roulette Wheel Selection

In roulette wheel selection [46], a roulette wheel is made up of all the individuals selected. The probability of a individual is proportional to its fitness value. That is, the larger the fitness value of a individual is, the greater the number of shares corresponding to that part of the roulette wheel will be. As can be seen from Figure 2, when the wheel stops after rotation, the pointer will randomly select, and the part that accounts for a large number of shares will have a great chance to be selected.

Of course, we can find that all the parts have the chance to be selected. The probability of selection can be expressed by mathematical formula as:

$$P_i = \frac{f_i}{\sum\limits_{j=1}^{n} f_i}, \tag{14}$$

where f_i indicates the fitness value of the i-th position.

The advantage of Roulette is that each individual is likely to be selected. Consequently, the diversity of the population is preserved. However, the selection mechanism of roulette still has some shortcomings:

1. Outstanding individuals will introduce a bias in the beginning of the search that may cause a premature convergence and a loss of diversity.
2. If the fitness values of individuals in a group are very similar, the selection probability of the better and the worse individuals is very close, so it is difficult for the group to develop in a better direction.
3. Many references have proved that this option is not suitable for minimization [47,48].
4. The algorithm procedure of roulette wheel selection depicted in Algorithm 2.

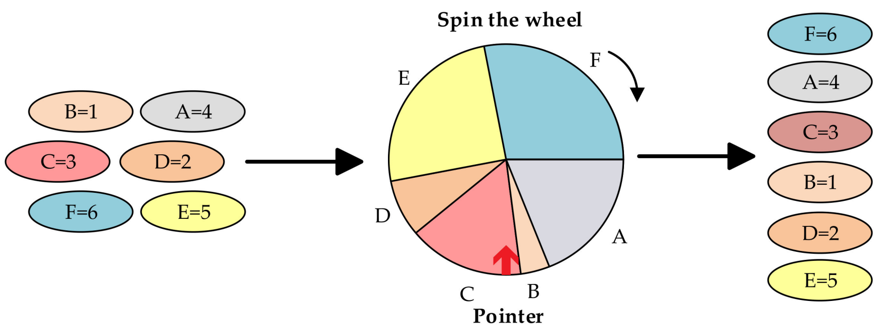

Figure 2. The roulette wheel selection.

Algorithm 2 Pseudo-Code of Roulette Wheel Selection

Procedure: Roulette wheel selection
  While population size<pop_size **do**
    Generate *pop_size* random number r
    Calculate cumulative fitness, total fitness, total fitness(Pi) and sum of proportional fitness (Sum)
      Spin the wheel *pop_size* times
        If $Sum < r$ **then**
          Select the first chromosome, otherwise, select j-th chromosome
        End If
    End While
  Return chromosomes with fitness value proportional to the size of selected wheel section
End Procedure

4.1.2. Tournament Selection

Tournament selection [49] is a mechanism similar to competition. The concept is quite simple and, with a probability of 68% in the confidence interval [50], a group of values (n) was randomly selected from the fitness function values (all participants) of all individuals in the population ($N, n \leq N$). Generate a random number $r, r \in [0, 1]$; according to the selection probability, generate the selection pressure p. The values in the selected group are compared (the contest), and the optimal value (the winner) is determined by the comparison of r and p. The optimal value is then substituted into the next iteration. Similarly, competition selection provides all individuals with the opportunity to compete fairly and the diversity of the population is preserved.

Tournament selection has several advantages:

1. Time complexity is more effective;
2. Not susceptible to optimal biasing;
3. No requirement for fitness scaling or sorting [45,48].

However, at the same time, there are also some shortcomings:

1. Suitable for small populations, large populations will lose diversity and fall into local optimum;
2. Relatively, slow convergence speed

Figure 3 illustrates this mechanism. Population size N is set to 8, and a group is randomly selected to participate in the competition. Membership size n is set to 3. Choose the optimal one through competition.

These two update mechanisms are different in principle. In this newly selected mechanism, a set of better values is selected according to the probability ratio among the existing fitness function values, and each selection is more focused on a better individual. The number of members in the group has a great influence on the optimal value selection, so we set an integer value ranging from 2 to the total number, called the tour parameters [51]. Here, we give the pseudo-code of tournament selection in Algorithm 3.

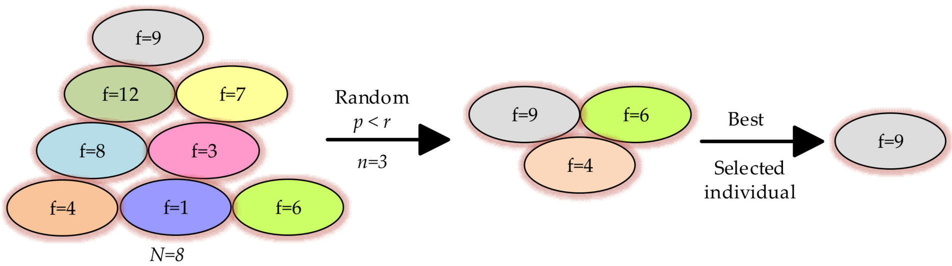

Figure 3. The tournament selection.

Algorithm 3 Pseudo-Code of Tournament Selection

```
Procedure: Tournament Selection
  Determine the population size N
    Generate the number of selected individuals n
      If i < n then
        Generate fitness values (Fi) for a set of selected individuals
      End If
    Select the minimum value in Fi and its corresponding index i
  Returns the individual with the minimum fitness value
End Procedure
```

4.2. *Lévy Flight*

Lévy flight is very common in nature, which is a kind of mathematical model of rapid flight, rapid jump. It is usually used to describe the behavior of birds, insects and other flying animals [52]. In the past few years, many studies have proved that it has great advantages in improving the convergence speed of the optimization algorithm and the convergence of the global optimal solution. Usually, it is considered as an operator that permits to enhance metaheuristic algorithms [53,54]. The mathematical model can be described as:

$$Levy(\lambda) = 0.01 \times \frac{\mu \times \sigma}{|\nu|^{\frac{1}{\beta}}}, \tag{15}$$

where μ and ν obey the normal distribution, $\lambda = \beta + 1$:

$$\mu \sim N(0, \sigma^2),\ \nu \sim N(0, \sigma_\nu^2), \tag{16}$$

with

$$\sigma = \left(\frac{\Gamma(1+\beta) \times \sin\left(\frac{\pi\beta}{2}\right)}{\Gamma\left(\frac{1+\beta}{2}\right) \times \beta \times 2^{\left(\frac{\beta-1}{2}\right)}} \right)^{\frac{1}{\beta}}, \sigma_\nu = 1. \tag{17}$$

The step length s can be expressed as:

$$s = \frac{\mu}{|\nu|^{\frac{1}{\beta}}}. \tag{18}$$

With the change of controlling parameter β, the shape of probability density function will also change, which will affect the shape of the tail region. Here, β is a constant, β = 1.5.

The selection strategy used in this paper, tournament selection, has the disadvantage of slow convergence. Lévy flight can be used as an operator for optimization improvement. In terms of global optimization of the algorithm, Lévy flight's occasional large leap can effectively avoid falling into local optimization.

4.3. Tournament-Based Lévy Multiverse Optimization Algorithm

In this paper, the MVO algorithm is improved by changing selection schemes, adding the random walk strategy and improving the updating formula, being aimed at improving the wide adaptability of the MVO algorithm to high dimensional multimodal optimization problems.

Tournament selection is the most effective when dealing with minimization issues [34,35]. In this regard, we invert the fitness value in the code for tournament selection. Adding the competition mechanism in the universe to better cooperate with black holes and white holes for material renewal between the universe. More effectively, the maximum fitness function value is screened out for the updating of the next generation.

For the location update of the optimal universe, we made several additional optimization improvements. Firstly, the current position is changed to the local optimal position. Secondly, taking the advantage of cuckoo algorithm in position updating, two arbitrary positions in any universe are randomly selected to make a difference (mutation factor). The diversity of the population would decline sharply in the later period. The introduction of this mutation factor and Lévy 's random walk strategy improves the development ability and maintains the diversity of the population [55].

The improved position update formula can be expressed as:

$$x_{i+1}^{j} = \begin{cases} \{x_{Best}^{j} + \{x_a - x_b \times r_3 + TDR \times \{\{ub_j - lb_j \times Levy + lb_j & r_2 < WEP \\ x_i^{j} & r_2 \geq WEP' \end{cases} \tag{19}$$

where x_{Best}^{j} represents the current optimal value, x_a, x_b indicate the position of two different objects in the universe, respectively:

$$TDR \times \left(\left(ub_j - lb_j\right) + lb_j\right). \tag{20}$$

This part has not changed much because this idea ensures that individuals can get random positions in the search space. In addition, the pseudo-code of the proposed algorithm shows in Algorithm 4.

Algorithm 4 Pseudo-Code of the Proposed Algorithm

```
Initialize the positions of universes;
Randomly initialize the population Sorted Universes (SU);
  While iteration < Max_iteration do
    For each universe indexed by i
      Check if any search agent goes beyond the search space and amend it;
      Calculate the reciprocal of the value of the objective function for each universe (1/Inflation_rates of the universe)(1/NI);
      Update the best solution Best_universe, and WEP and TDR;
        For each object indexed by j
  Using Tournament Selection methods and the idea of wormhole, white hole, and black hole to update the universe using Equation (10)
   Update the position of object in the optimal universe using Equation (19)
     End for
   End for
 End while
```

4.4. The Proposed TLMVO-Based Multilevel Thresholding Method

Combining the TLMVO algorithm with a multilevel threshold method, Masi entropy is taken as the objective function. By determining the maximum entropy between classes, the corresponding optimal threshold is obtained, so as to obtain better image segmentation results. The position of the individual is determined by multiple thresholds, and different individuals make up the universe. The inflation rate of universe corresponds to the value of the objective function, thus establishing the relationship between the optimization algorithm and segmentation function.

From the overall perspective of the program, the individual and other related parameters are initialized, calculate the initial fitness function values with formulas Equations (6) and (7). The fitness function value is screened through the tournament selection mechanism, determine the optimal individual, and exchange individuals between the universe. Under the triple constraint of individual range Equation (20), wormhole existence rate (WEP) Equation (12), travel distance rate (TDR) Equation (13) and Lévy Flight Equation (15), the optimal universe was updated with formula Equation (20). The iterative loop determines the optimal threshold and completes the image segmentation. The overall flow chart is shown in Figure 4.

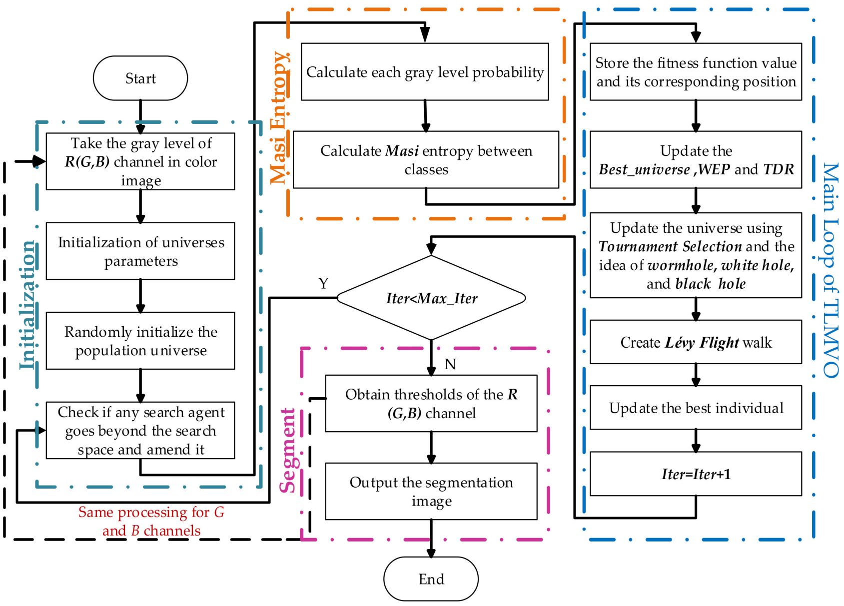

Figure 4. The flow chart of the TLMVO-based multilevel thresholding method.

5. The Computational Experiments and Results

In order to evaluate the performance of the algorithm, computational experiments were carried out on the convergence curve of the segmentation function and the evaluation index of image segmentation effect. The general structure is as follows: Section 5.1 briefly introduces the basic experimental environment; the measured images, comparison algorithm and related parameters are given in Section 5.2; in Section 5.3, several performance measures are chosen to evaluate the segmentation effect; the experimental data are analyzed in Section 5.4 finally.

5.1. Experimental Setup

The computer is configured with Intel(R) Pentium(R) CPU G4560@3.50 GHz (Intel, Santa Clara, CA, USA), Microsoft Windows 7 system (Microsoft, Redmond, WA, USA), and the operating environment is Matlab R2017b (The MathWorks Inc., Natick, MA, USA).

The proposed method is compared with several well-known metaheuristicss algorithms. Each of them contains different characteristics, including

1. The traditional MVO algorithm [30];
2. The state-of-the-art LMVO algorithm [37];
3. An interesting bionic algorithm named ant lion algorithm (ALO) which can always find the maximum in the latest metaheuristics algorithm [56];
4. A new complex swarm intelligent optimization technology, dragonfly algorithm (DA) [43];
5. FPA, inspired by the process of flower pollination of flowering plants in nature which is simple and requires fewer parameters to be adjusted [41,42];
6. An earlier proposed evolutionary algorithm, PSO [57–60];
7. CS which is based on the brood parasitism of some cuckoo species, along with Lévy flights' random walks [39,40].

The seven comparison algorithms correspond to four relatively novel algorithms and three relatively basic algorithms, respectively. The parameters of these algorithms are selected from the references related to image segmentation, which are shown in Table 1.

Table 1. Parameters of algorithms.

Reference	Algorithm	Parameters	Value
[30]	MVO [1]	Mining capability p Random parameters r_1, r_2, r_3, r_4 Contrast parameter H	1/6 [0,1] 0.5
[37]	LMVO [1] TLMVO [1]	Lévy controlling constant β Selection pressure p Screening probability r	1.5 [0,1] [0,1]
[61]	ALO	Switch possibility	0.5
[44]	DA	Inertial weight Seperation weight Alignment weight Cohesion weight	[0.5,0.9] [0,0.2]
		Maximum velocity Food attraction weight Enemy distraction weight	25.5 [0,2] [0,0.1]
[43]	FPA	Switch possibility Lévy controlling constant β	0.4 1.5

Table 1. *Cont.*

Reference	Algorithm	Parameters	Value
[59]	PSO	Maximum inertia weight	0.9
		Minimum inertia weight	0.4
		Learning factors c_1 and c_2	2
		Maximum velocities	+120
		Minimum velocities	−120
[7]	CS	Mutation probability value P_a	0.25
		Scale factor β	1.5

[1] As an improvement of the algorithm, the same parameters are not given repeatedly.

Comparative experiments were conducted using control variable method. The maximum number of iterations for all algorithms is 500 and the number of population size is 25. For each image, each algorithm runs 30 times separately. The threshold dimension of K is divided into high dimension (K = 10, 12) and low dimension (K = 4, 6, 8).

5.2. Satellite Color Image Used

This paper presents a new improved TLMVO algorithm for satellite image segmentation using Masi entropy. In satellite images, there are different bands and different wavelength areas. The processing of satellite images is carried out in different wavebands (the full band combination specifications are presented in Table 2. Secondly, the image features are very dense and the information from one area to another changes rapidly. At the same time, satellite images are generally of high resolution. All these will affect the efficiency of the algorithm, which will lead to inefficiency of the algorithm and increase the amount of computation in segmentation. Therefore, the accurate segmentation of satellite images is a very challenging task [5].

Table 2. Characteristics and Use [4].

Band No.	Name	Wavelength (µm)	Characteristics and Use
1	Visible blue	0.45–0.52	Maximum water penetration
2	Visible green	0.52–0.60	Good for measuring plant Vigor
3	Visible red	0.63–0.69	Vegetation discrimination
4	Near infrared	0.76–0.90	Biomass and shoreline Mapping
5	Middle Infrared	1.55–1.75	Moisture content of soil
6	Thermal Infrared	10.4–12.5	Soil moisture, thermal mapping
7	Middle Infrared	2.08–2.35	Mineral mapping

Ten satellite images are selected for segmentation to achieve better contrast effect. Each threshold has a range of $[0, 256)$, and thus the search space is $[0, 256)^{25}$. The size and histogram of each satellite image are presented in Figure 5, which are from the aerial data set [62]. For each color image and threshold level, 30 independent running experiments were conducted [63,64]. The corresponding thresholds for each optimal solution are reported in Table 3.

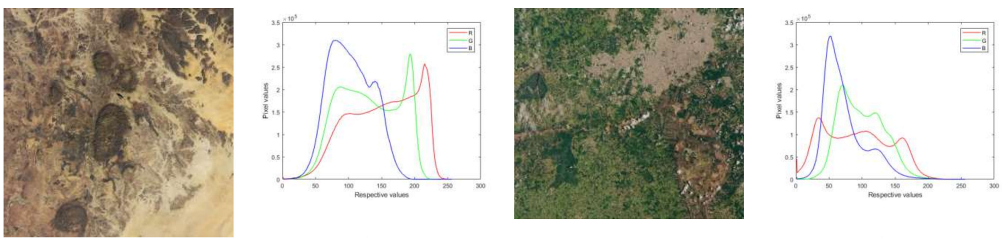

Image1: 5241×5241
Airmountains oli

Image2: 4180×3847
Brazilminecollapse oli

Figure 5. *Cont.*

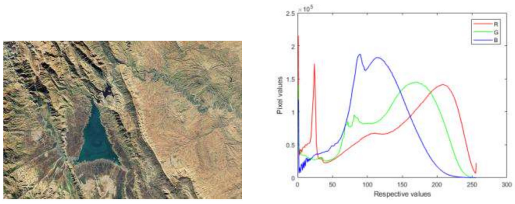

(a) **(b)**

Image3: 5339×3559

The Lake Dukan situated in the Zagros Mountains

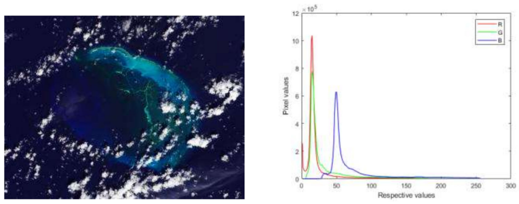

(a) **(b)**

Image4: 3601×2742

Eastisland oli

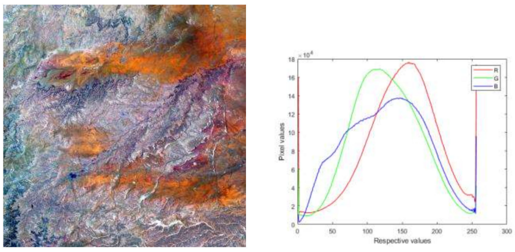

(a) **(b)**

Image5: 4627×4627

Gaara oli

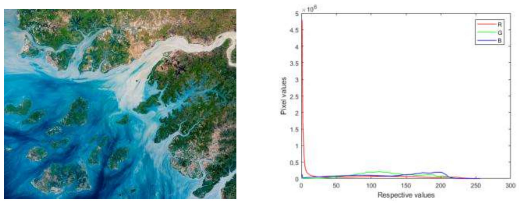

(a) **(b)**

Image6: 5130×4203

The Meandering Estuaries of Guinea - Bissau

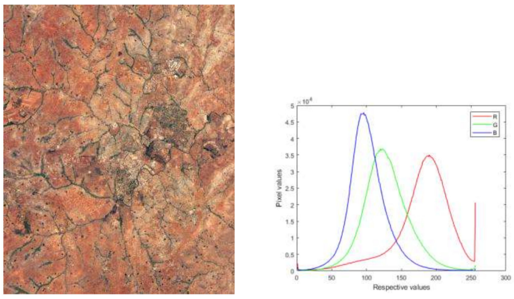

(a) **(b)**

Image7: 1440×1800

The Malawian capital of Lilongwe

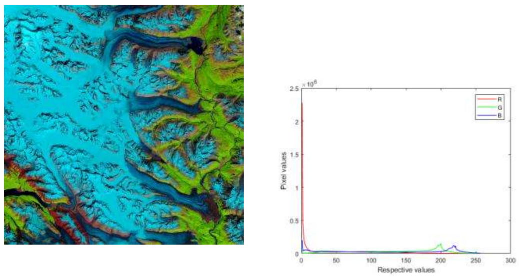

(a) **(b)**

Image8: 2718×2718

Lowell msi

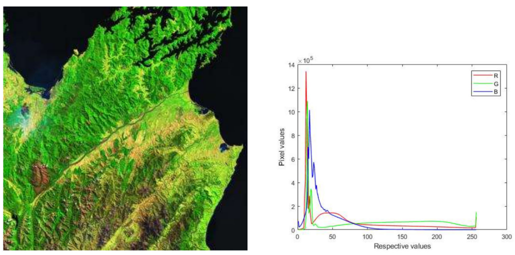

(a) **(b)**

Image9: 4096×4096

Newzealand oli

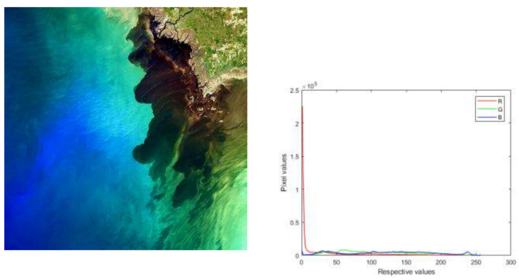

(a) **(b)**

Image10: 936×936

A Blackwater River Meets the Sea

Figure 5. The experimental satellite images and corresponding histogram images.

Table 3. Optimal solution for each algorithm under Masi entropy.

TEST IMAGES	K	TLMVO			LMVO			MVO			ALO			DA			FPA			PSO			CS		
		R	**G**	**B**	**R**	**G**	**B**	**R**	**G**	**B**	**R**	**G**	**B**	**R**	**G**	**B**	**R**	**G**	**B**	**R**	**G**	**B**	**R**	**G**	**B**
1	**4**	57 100 140 182	50 93 131 168	43 83 121 158	57 100 140 182	56 98 138 173	43 83 122 163	57 100 143 181	56 98 138 173	43 83 121 158	57 100 140 182	56 98 138 173	43 83 122 163	57 103 142 184	56 98 138 173	43 81 121 158	71 119 170 205	50 69 106 158	46 84 115 164	57 100 140 182	56 98 138 173	43 83 122 163	54 93 138 183	48 103 138 180	47 91 117 166
	6	57 80 111 142 172 202	50 81 112 144 175 205	43 74 103 130 163 229	55 76 107 139 172 202	47 65 99 134 166 203	38 57 88 121 152 171	57 80 111 141 172 202	46 64 93 122 151 180	38 57 85 112 139 166	57 80 111 142 172 202	50 81 112 144 175 205	38 57 85 113 140 166	57 82 114 144 175 203	46 64 93 122 152 180	38 57 85 112 139 166	60 72 88 132 142 169	42 57 94 115 128 157	22 60 107 124 143 171	57 80 111 142 172 202	46 64 93 123 152 180	40 63 90 117 143 166	54 99 117 139 169 186	54 90 114 140 165 181	39 83 104 117 140 172
	8	54 70 94 119 145 172 200 227	37 50 66 90 114 138 160 183	38 55 77 100 123 148 167 230	46 64 82 103 127 150 177 203	46 61 84 107 131 155 180 205	38 49 67 88 109 130 152 171	55 72 94 117 139 162 184 206	46 59 80 102 127 152 180 205	38 52 71 91 112 133 154 171	46 64 84 108 132 156 180 206	46 63 87 110 134 157 181 205	38 53 72 92 113 134 155 171	54 70 94 118 141 164 186 208	43 57 78 98 120 155 180 205	38 53 74 95 116 136 155 171	47 51 70 84 120 147 191 212	35 43 54 66 93 122151 182	40 46 63 69 106 135 157 214	46 64 84 108 131 156 180 205	46 61 85 109 134 158 182 205	38 53 74 94 114 134 155 171	44 60 85 117 132 160 194 210	43 63 83 107 130 140 160 200	46 61 81 102 113 125 135 161
	10	46 57 67 81 99 117 135 156 179 205	41 56 71 89 107 125 144 163 183 205	38 52 68 85 103 120 137 155 171 184	46 63 79 97 115 133 152 171 189 208	37 50 63 82 101 120 140 161 182 205	33 46 64 85 107 129 154 171 206 208	46 63 77 93 112 131 151 170 189 208	41 56 68 84 102 118 136 158 181 205	33 46 60 77 94 110 123 138 155 171	46 64 80 97 115 133 151 171 191 210	41 56 71 90 108 127 145 164 183 205	33 46 58 74 91 107 124 141 156 171	55 72 91 112 132 151 171 189 207 227	41 56 70 88 106 120 137 160 183 206	38 49 65 80 96 111 126 141 156 171	39 53 81 97 97 107 127 160 188 206	40 50 71 82 97 119 140 154 190 227	25 40 51 60 74 100 101 127 147 176	46 64 82 104 126 146 167 187 206 227	41 56 71 89 107 125 144 163 184 205	33 46 59 74 90 106 122 139 155 171	44 54 62 88 99 115 157 168 193 210	39 52 61 77 92 101 126 135 159 167	30 39 66 73 79 109 123 136 146 164
	12	46 57 67 82 99 115 132 149 167 186 205 227	41 56 68 84 100 116 132 148 164 181 197 207	23 33 41 50 62 76 90 106 122 138 155 171	46 63 76 89 105 122 139 155 172 189 207 227	37 47 57 69 84 99 115 132 149 166 184 205	33 46 57 70 84 98 112 126 140 155 171 184	46 63 76 91 105 119 135 153 175 191 208 227	37 50 62 78 95 113 130 146 161 175 188 205	30 40 50 63 77 92 107 122 135 149 163 173	46 57 73 96 116 136 155 171 184 198 212 227	37 48 61 77 93 110 126 140 155 169 187 205	33 43 56 69 82 94 106 117 129 141 156 171	46 57 67 87 107 125 142 159 177 193 210 227	43 56 68 83 99 114 130 148 165 181 197 207	30 43 55 71 87 103 114 126 138 152 163 173	64 74 85 91 95 120 133 143 156 173 182 197	44 58 65 84 87 97 108 112 129 150 164 181	19 30 40 45 57 62 71 106 122 147 168 183	46 57 73 91 110 129 147 168 188 207 227 256	37 50 63 80 96 111 126 140 155 171 186 205	1 33 44 57 71 86 101 116 130 144 158 171	42 48 59 70 93 103 120 142 161 178 190 205	47 53 61 69 82 92 99 119 128 154 174 189	39 45 49 67 72 92 107 118 155 164 167 171
2	**4**	60 117 174 197	38 80 123 170	33 88 141 170	60 117 174 197	59 117 157 187	33 88 141 170	50 88 126 182	38 111 157 187	44 89 141 170	50 88 126 182	59 117 157 187	33 88 141 170	50 89 126 182	63 117 157 187	33 88 141 177	67 84 116 195	64 115 164 213	58 95 138 178	58 95 138 178	38 111 157 187	33 88 141 170	41 77 120 179	58 117 157 184	51 94 148 187
	6	30 61 94 127 174 197	38 63 93 124 158 187	19 46 88 135 158 193	43 81 121 172 190 212	38 61 91 123 157 187	19 46 88 135 157 181	35 69 105 137 174 197	38 6192 123 158 187	19 46 82 109 141 170	35 69 106 138 174 197	38 63 93 124 158 187	19 46 82 109 141 170	42 76 112 143 177 205	38 63 95 125 160 189	27 59 93 141 168 193	51 80 97 135 176 186	51 96 111 160 191 214	36 91 116 148 173 185	30 68 106 138 177 205	38 63 93 124 160 189	19 46 88 135 157 181	40 73 114 142 173 191	33 42 77 122 162 194	25 68 99 139 169 187
	8	23 50 79 112 141 172 190 212	36 55 78 103 127 155 174 202	19 44 75 101 135 157 177 197	18 42 68 94 120 147 177 205	36 57 81 105 128 157 179 208	19 46 78 103 135 157 177 203	23 46 71 95 120 146 177 205	36 56 80 104 127 155 174 202	17 33 57 83 108 136 157 181	30 61 90 118 145 172 190 212	38 59 83 106 130 157 177 208	17 34 59 85 109 136 157 185	39 66 95 120 146 172 190 212	36 58 82 107 130 157 179 208	19 46 76 101 133 149 170 193	42 69 100 123 134 149 186 212	39 45 80 105 133 166 208 211	25 33 46 56 90 139 160 195	30 58 87 117 144 172 190 212	38 59 83 107 130 157 177 208	19 46 78 102 133 149 170 197	19 61 75 104 119 142 170 190	37 59 91 108 138 160 178 203	18 35 71 98 127 144 161 194
	10	17 37 59 82 105 126 148 172 190 212	17 37 59 82 105 126 148 172 190 212	17 33 56 80 102 128 141 157 178 203	22 42 63 84 106 126 148 172 190 212	32 44 59 80 101 125 152 168 187 208	17 32 52 74 93 113 136 157 177 203	17 35 57 81 103 126 149 174 190 212	36 52 68 86 104 121 138 157 177 202	17 31 49 69 91 111 133 149 170 193	17 37 60 83 105 126 149 172 190 212	32 48 67 87 108 129 154 170 187 208	17 34 57 81 102 128 141 159 178 203	17 34 57 81 102 128 141 159 178 203	38 59 86 110 136 155 170 187 208 224	19 33 53 74 94 115 137 157 178 203	17 48 78 128 144 163 168 181 187 216	24 59 68 102 113 125 152 162 173 196	25 33 41 59 66 93 125 147 184 210	18 39 61 83 106 128 150 174 190 212	36 53 73 95 114 134 155 170 189 208	17 33 53 74 93 113 134 149 170 193	31 44 61 79 96 111 135 171 202 210	23 36 61 77 108 121 153 177 208 220	34 54 82 122 136 143 150 162 172 197
	12	9 22 37 54 70 88 107 126 149 174 190 212	26 38 53 72 91 112 132 154 169 187 202 218	17 32 50 70 89 108 128 141 157 175 193 210	9 22 36 52 74 97 121 145 169 182 197 212	26 38 52 66 83 101 119 135 154 168 187 208	11 25 39 58 82 103 127 141 157 172 191 208	17 30 47 68 87 105 123 139 153 172 190 212	26 38 53 69 86 104 121 136 153 168 187 208	11 19 32 50 73 92 111 131 145 164 181 203	17 35 55 72 93 110 132 151 170 182 197 212	32 44 61 78 95 113 130 149 160 174 189 210	17 31 46 63 79 96 113 131 144 160 179 203	17 34 53 72 89 107 124 138 153 174 190 212	36 50 65 80 97 119 139 155 170 187 205 220	17 28 44 60 78 96 116 133 145 160 179 203	5 4 58 64 83 114 138 146 173 197 221 239	32 72 85 98 101 126 152 171 174 182 209 227	20 26 46 61 76 92 112 119 137 143 167 191	11 28 47 66 84 102 120 137 154 174 190 212	26 38 53 69 86 103 120 137 155 170 189 210	17 32 48 66 82 99 115 134 149 170 197 256	19 54 78 90 109 118 135 175 184 200 212 237	17 32 56 67 90 105 125 138 160 168 175 194	19 41 62 71 77 83 102 116 131 142 157 166

Table 3. *Cont.*

TEST IMAGES	K	TLMVO			LMVO			MVO			ALO			DA			FPA			PSO			CS		
		R	G	B	R	G	B	R	G	B	R	G	B	R	G	B	R	G	B	R	G	B	R	G	B
3	4	69 109 158 212	55 96 137 185	36 68 108 156	69 109 158 212	30 63 121 185	59 102 144 176	69 109 158 212	55 94 136 185	57 99 144 176	75 117 163 212	55 96 137 185	43 78 144 176	72 114 162 212	59 100 140 185	59 102 144 176	70 126 168 208	26 61 122 201	54 76 137 169	75 117 163 212	59 99 138 185	43 78 141 176	79 130 165 217	58 103 148 192	61 93 141 175
	6	36 68 100 137 174 214	55 87 119 151 185 213	26 54 79 112 148 176	36 68 100 137 174 214	30 63 100 136 173 204	30 57 81 113 148 176	36 68 100 135 173 214	30 62 96 132 170 198	36 67 96 124 151 177	36 68 100 137 174 214	30 63 100 136 175 204	26 57 81 113 148 176	40 75 109 145 182 217	33 63 100 136 173 204	36 67 96 124 151 177	19 84 100 155 180 213	51 69 81 124 159 194	27 63 89 122 140 170	36 68 100 137 174 214	30 63 99 134 170 198	32 59 83 114 148 176	50 75 125 153 186 225	27 58 72 100 135 186	42 72 93 115 135 177
	8	16 39 69 99 130 161 193 221	19 40 63 92 121 149 180 204	19 39 59 79 104 129 153 177	34 62 86 112 140 170 206 231	19 40 63 92 121 151 185 213	24 47 70 93 116 141 163 181	35 62 87 117 146 176 209 231	30 61 85 111 138 165 189 213	24 46 68 92 116 141 163 181	35 65 93 121 150 179 209 231	30 61 87 112 138 165 189 213	24 47 70 93 117 141 163 181	16 40 70 100 135 169 206 231	30 61 86 112 138 165 189 213	25 49 72 96 119 143 163 181	14 76 110 131 164 178 202 232	9 37 52 81 104 136 182 203	27 54 74 84 106 130 142 192	16 43 75 106 139 172 206 231	30 61 87 115 142 170 192 213	24 46 68 91 116 141 163 181	12 55 90 100 148 175 205 223	23 68 104 137 153 171 197 214	44 71 110 122 137 149 165 177
	10	16 35 62 85 107 131 156 183 212 232	18 3 61 80 102 124 146 170 192 213	19 37 57 74 94 113 133 151 168 183	16 35 62 85 109 134 160 186 212 232	18 38 60 79 100 122 146 170 192 213	15 32 51 68 85 104 124 144 163 181	16 35 61 83 104 130 157 183 210 231	16 38 60 81 102 125 147 170 192 213	19 36 54 71 90 109 129 148 168 183	16 35 62 86 110 134 161 187 212 232	18 39 62 83 105 126 149 173 192 213	19 39 59 76 96 115 134 151 168 184	16 39 68 95 121 147 173 198 221 239	19 43 63 83 107 128 149 172 192 213	19 37 57 74 93 113 132 150 168 184	44 65 73 85 98 134 176 202 217 232	22 42 61 79 102 111 128 142 176 201	28 57 84 93 97 110 133 140 147 193	16 36 62 86 110 136 162 187 212 232	18 38 61 82 104 126 148 171 192 213	19 39 59 78 96 115 134 151 168 184	15 31 64 90 119 151 162 173 202 222	33 63 76 98 134 146 159 193 210 219	44 60 73 96 106 117 132 145 161 180
	12	16 32 50 68 86 106 125 145 166 188 212 231	18 38 59 76 93 110 127 144 162 180 196 213	18 35 52 68 83 99 115 131 148 163 176 187	16 32 50 68 86 107 128 149 170 191 212 231	14 30 48 63 79 96 113 131 149 171 192 213	15 29 45 61 78 96 114 132 151 168 183 246	16 30 46 65 83 100 119 138 159 182 210 231	18 36 52 66 84 103 121 139 158 178 196 213	15 32 51 65 80 96 112 128 146 163 176 187	16 34 55 75 97 117 139 159 180 202 221 239	18 38 60 79 97 114 131 149 168 186 204218	19 36 53 68 83 101 118 136 152 168 184 237	16 34 57 77 98 120 141 161 188 206 222 239	16 34 55 71 90 106 125 145 165 185 204 218	19 38 54 70 86 103 118 133 148 163 176 187	17 31 39 64 80 138 167 176 198 218 232 240	18 33 44 52 69 76 99 124 138 154 169 192	26 32 44 58 83 98 123 143 162 170 181 191	16 34 54 75 95 117 139 161 183 204 221 237	18 38 61 79 97 115 133 151 169 186 204 218	19 36 53 68 83 99 115 131 148 163 176 187	17 38 49 65 84 100 120 152 162 194 219 240	34 45 62 79 101 124 143 161 178 185 191 219	21 35 46 59 73 80 100 110 113 127 157 177
4	4	35 80 135 195	36 83 140 197	40 77 124 180	35 80 135 195	34 74 128 190	77 119 169 212	35 80 135 195	34 74 128 190	77 119 169 212	35 80 135 195	36 83 140 197	77 119 169 212	35 80 141 199	34 74 128 192	77 119 169 212	38 103 157 195	31 83 165 195	77 134 167 204	35 80 135 195	36 83 140 197	77 119 169 212	37 69 124 195	40 79 134 186	72 108 165 223
	6	25 61 103 141 179 217	34 71 106 142 179 217	61 88 119 151 184 219	25 58 94 134 174 215	31 62 93 128 167 208	40 65 95 133 174 214	25 61 103 141 178 216	34 69 104 140 176 216	40 65 95 133 176 216	25 58 95 135 175 215	34 71 106 142 180 218	40 65 95 133 176 216	25 61 103 141 179 217	34 71 111 147 183 220	40 65 96 135 180 217	26 61 107 148 200 212	24 50 88 121 181 220	32 92 141 173 200 234	25 61 103 141 179 217	34 71 106 142 179 217	40 65 95 133 174 215	23 68 99 137 167 218	27 66 105 156 181 208	36 61 95 123 152 196
	8	23 46 73 103 133 164 195 225	24 47 73 103 132 162 193 224	40 63 88 115 144 174 200 228	23 46 73 104 134 164 194 225	24 47 73 103 132 162 193 224	40 63 88 117 145 174 200 227	23 46 72 103 131 159 190 223	24 47 73 103 132 162 194 225	40 63 88 115 145 174 200 228	22 43 72 104 135 166 196 226	31 58 84 112 140 168 197 225	40 63 88 116 142 169 197 226	24 50 80 111 142 171 199 227	31 62 89 117 144 175 203 232	40 63 88 117 146 174 201 229	49 66 85 113 144 156 179 194	34 71 106 141 149 172 183 218	28 46 90 97 110 153 196 224	23 46 73 104 134 164 195 225	31 58 84 112 140 168 197 227	40 63 88 115 142 169 199 226	25 36 63 99 133 159 211 232	35 55 63 107 139 166 207 236	35 81 116 140 169 187 221 238
	10	22 40 60 82 104 125 148 174 200 228	10 31 55 78 103 128 154 179 205 231	26 41 57 76 96 119 142 169 195 223	22 43 70 94 118 140 163 186 208 231	24 47 71 93 116 140 162 185 208 232	26 41 60 81 103 126 151 176 200 227	22 42 61 83 105 129 152 176 202 230	22 39 62 83 106 129 154 177 202 229	40 58 77 96 118 140 162 184 207 229	23 43 70 94 118 141 163 187 209 233	23 43 67 91 115 138 162 185 208 232	26 41 60 84 107 129 152 176 201 229	22 43 70 95 119 142 164 187 210 233	23 44 69 92 117 140 162 184 208 232	41 65 92 121 145 169 189 206 223 240	7 26 46 66 84 136 146 179 206 240	10 24 56 89 102 116 124 167 200 216	23 40 93 113 144 149 176 183 207 235	22 42 63 84 107 132 158 182 206 231	9 24 47 73 102 128 154 180 206 231	26 41 60 84 107 129 152 176 202 229	21 41 58 68 79 103 138 166 174 191	24 41 72 127 160 178 188 206 221 246	27 45 69 86 109 141 161 174 196 230
	12	22 40 61 82 103 121 141 160 179 198 217 237	9 22 38 58 78 99 119 140 162 185 208 232	40 58 77 95 113 132 151 169 184 201 218 236	21 35 52 71 91 110 130 151 171 191 212 234	22 39 59 78 98 118 139 159 178 197 216 236	26 41 56 76 94 113 133 153 174 194 214 234	21 37 54 72 90 108 129 149 170 191 212 234	22 38 55 73 91 110 129 149 169 191 212 234	26 41 56 75 93 111 131 151 173 193 213 234	22 42 61 80 100 119 139 159 178 198 218 237	23 41 60 80 100 119 139 159 178 198 217 237	26 41 56 73 89 108 127 147 169 191 212 234	22 40 61 82 104 127 149 169 188 206 224 240	23 41 62 82 102 121 140 160 179 199 219 238	26 41 59 79 101 124 151 176 198 216 230 242	14 35 50 72 86 90 137 163 176 188 204 222	52 73 86 96 113 131 152 164 185 192 212 222	20 34 50 54 74 80 94 129 144 162 214 238	22 42 61 80 100 119 139 158 178 199 219 239	9 23 41 62 83 105 126 147 168 191 213 234	1 26 41 60 80 102 124 147 169 190 212 233	33 43 56 92 111 126 133 149 156 176 211 226	25 48 91 112 127 146 171 193 203 225 233 246	17 36 61 74 105 113 135 153 170 183 200 221

Table 3. *Cont.*

TEST IMAGES	K	TLMVO			LMVO			MVO			ALO			DA			FPA			PSO			CS		
		R	G	B	R	G	B	R	G	B	R	G	B	R	G	B	R	G	B	R	G	B	R	G	B
5	4	54 88 139 203	46 86 169 217	64 121 189 226	43 88 139 203	53 103 173 217	62 116 170 215	54 88 139 203	46 86 169 217	64 121 189 226	46 88 139 203	53 104 175 217	64 121 189 226	57 100 171 214	48 98 169 217	65 124 189 226	54 104 172 205	52 118 175 226	54 118 171 221	54 88 139 203	53 104 175 217	64 121 189 226	47 89 137 212	58 111 165 217	84 131 179 224
	6	34 68 101 142 187 223	39 77 117 159 195 221	34 73 113 154 194 226	43 85 118 158 196 224	38 72 112 155 192 220	34 73 113 154 194 226	34 65 100 140 187 223	38 72 112 155 192 220	38 74 114 154 194 226	34 68 101 139 180 214	39 75 114 155 192 220	38 76 116 156 194 226	34 69 103 143 187 223	39 77 117 159 195 221	34 73 116 156 194 226	50 86 105 126 181 210	28 55 75 119 153 206	33 52 71 118 159 210	34 65 100 141 187 223	39 77 117 159 195 221	38 76 116 156 194 226	44 80 128 160 205 235	55 91 127 169 199 234	35 77 109 132 198 228
	8	29 57 86 112 143 175 202 227	26 48 74 102 132 165 195 221	24 56 86 116 147 178 205 227	34 61 88 115 145 175 202 227	26 52 79 110 141 173 202 226	22 51 81 112 142 173 203 227	34 58 88 116 144 175 203 232	26 48 76 102 130 164 195 221	22 50 78 108 140 172 203 226	29 57 86 111 142 175 202 227	26 52 79 114 145 175 202 226	34 62 90 119 149 179 205 227	29 58 88 116 147 178 203 228	26 53 83 116 150 181 206 234	24 56 87 119 148 178 205 227	23 46 75 118 144 180 217 227	29 61 74 119 151 194 230 239	35 89 106 157 182 196 210 234	29 58 88 116 145 175 202 227	26 53 82 114 147 178 206 234	24 56 85 114 144 174 203 227	26 46 79 101 140 169 203 231	18 35 50 85 112 149 185 221	31 54 93 107 156 187 205 231
	10	21 43 65 88 111 138 165 190 214 235	26 45 65 90 116 142 169 195 215 234	18 39 63 87 111 135 160 186 208 231	20 43 65 88 110 135 161 187 209 232	22 39 61 82 106 134 161 188 213 234	15 34 59 83 108 133 159 186 208 231	21 43 65 88 108 130 153 180 203 230	25 43 63 85 112 140 165 191 213 234	17 38 60 83 106 130 157 184 208 231	21 43 65 88 112 139 165190 212 235	26 48 73 97 121 146 167 192 213 234	18 41 65 90 115 140 165 191 213 232	30 57 85 107 130 155 178 201 221 239	26 48 75 102 128 153 178 198 217 238	18 43 71 99 127 154 176 198 215 235	29 52 78 112 126 131 161 176 204 222	42 75 93 106 114 128 145 176 227 244	8 32 61 71 97 124 153 188 216 229	21 43 65 88 112 138 165 190 214 235	26 48 73 98 123 149 175 198 217 234	18 39 64 89 114 139 163 188 210 231	6 26 64 89 116 142 150 175 204 224	48 66 80 88 113 143 151 184 206 230	18 43 54 98 113 136 154 165 187 213
	12	18 34 54 71 88 109 132 155 180 202 223 239	25 43 63 84 106 129 152 175 195 213 226 242	11 22 37 53 72 92 114 137 162 186 208 231	14 29 43 60 77 93 112 133 154 178 203 232	25 42 61 81 102 123 143 163 182 202 219 238	17 34 54 74 94 114 135 155 176 196 215 235	19 36 54 69 88 107 129 151 174 195 214 235	22 38 55 75 94 120 139 158 177 196 215 234	11 28 47 65 86 105 127 148 171 194 213 231	21 42 61 80 99 119 140 161 182 203 223 240	25 43 63 83 103 123 143 164 183 202 217 234	17 34 53 72 91 112 133 153 172 194 213 232	28 47 65 85 103 121 139 159 180 198 216 235	26 43 64 83 99 115 135 155 175 195 217 238	17 38 60 83 107 130 150 169 186 203 218 235	14 47 66 80 97 127 147 188 208 220 224 246	31 47 63 81 100 114 125 165 185 205 226 247	16 33 77 87 101 119 130 142 157 213 229 238	21 43 62 82 101 121 141 161 181 202 223 240	25 39 55 76 97 117 138 159 179198 217 234	14 34 53 73 94 114 134 154 174 194 215 235	36 49 59 84 112 122 129 153 170 196 229 241	21 31 66 80 101 124 142 156 185 193 219 246	42 52 77 97 117 137 167 175 188 196 207 234
6	4	25 75 127 175	45 81 128 170	38 84 129 172	25 75 127 175	45 81 128 170	38 84 129 172	25 75 127 175	45 81 129 172	38 84 129 172	25 75 127 175	45 81 129 172	38 84 129 172	25 75 127 175	45 81 130 175	38 34 129 172	37 95 137 173	35 54 122 158	27 82 118 173	25 75 127 175	45 81 129 172	38 84 129 172	24 81 123 169	47 72 132 173	42 84 128 174
	6	16 54 90 12 163 197	42 68 98 129 159 192	27 56 87 118 149 182	16 53 89 127 163 197	40 63 93 127 159 192	22 51 83 116 149 182	16 52 88 126 163 197	42 68 97 128 158 192	27 56 87 118 149 182	16 54 91 128 163 197	42 68 98 129 159 192	27 56 87 118 149 182	20 59 96 133 168 199	42 70 99 129 159 192	27 56 87 119 151 183	6 50 95 124 177 218	50 72 88 108 144 169	16 53 73 96 119 155	16 54 91 128 163 197	42 68 98 129 159 192	26 56 87 118 149 182	16 33 62 91 131 190	32 64 90 116 147 179	35 68 82 104 133 171
	8	15 41 67 94 121 147 174 202	37 58 79 102 126 149 172 195	13 35 59 85 110 136 162 189	15 45 75 105 136 168 197 226	34 52 74 96 119 143 167 193	21 43 68 93 118 143 168 193	15 40 66 92 119 146 173 202	36 54 75 99 124 147 170 194	21 43 67 90 114 139 165 190	15 41 68 95 122 148 175 202	37 54 75 99 124 146 169 193	21 4 67 91 116 140 165 190	15 41 70 98 125 152 177 204	40 59 80 103 126 148 171 194	21 43 68 92 117 141 167 193	24 48 64 97 137 189 200 224	18 40 65 89 106 111 122 171	26 58 86 150 162 191 206 221	15 41 68 95 122 148 175 202	40 59 80 103 126 149 172 195	21 43 68 93 118 143 168 193	16 44 85 102 125 175 186 211	48 87 102 127 159 172 184 204	26 47 62 83 100 117 130 183
	10	10 27 46 64 85 109 135 162 187 212	34 52 71 90 109 128 148 168 188 207	13 31 48 68 89 110 131 157 184 219	12 32 52 74 95 117 143 170 197 226	32 45 59 74 92 113 135 158 189 218	13 31 50 71 92 114 136 160 186 219	12 33 54 76 99 121 143 166 187 210	34 47 63 80 98 118 138 157 176 196	13 31 51 71 91 111 133 154 175 197	13 36 59 82 104 126 148 170 191 214	34 52 72 92 113 134 154 173 195 219	13 31 51 74 95 116 137 157 177 198	16 46 78 102 127 148 170 193 212 231	36 54 74 94 115 135 157 176 196 219	13 31 51 72 93 114 135 157 179 201	18 45 83 98 106 142 175 210 217 232	20 37 50 73 83 106 124 134 163 210	18 48 70 90 117 133 151 189 195 214	13 35 57 79 102 124 146 168 190 212	34 52 72 91 110 129 148 168 188 207	17 35 55 75 95 115 135 155 176 198	13 28 58 75 93 109 140 170 195 208	36 43 59 79 105 117 128 140 164 182	26 53 64 82 104 126 137 159 169 194
	12	11 29 49 69 89 108 128 148 168 187 207 231	32 45 59 74 89 105 122 138 154 171 189 207	7 17 29 43 58 75 92 111 131 150 172 195	12 32 52 71 90 110 129 148 168 187 206 226	34 47 63 79 96 114 133 152 173 194 218 244	17 33 51 69 87 106 125 144 162 180 199 219	10 27 46 64 81 101 119 138 159 180 202 226	34 47 61 75 91 108 124 140 158 177 196 219	13 27 45 63 82 102 123 142 160 180 199 219	11 30 49 68 89 111 131 150 169 187 206 226	34 47 63 79 95 112 129 146 163 181 199 219	13 31 50 70 89 108 128 145 163 180 198 219	11 30 50 70 90 110 129 147 165 183 204 226	34 47 62 79 97 118 138 158 174 191 206 219	13 27 48 69 89 109 130 151 168 185 202 219	16 29 35 49 89 96 107 128 163 190 210 239	38 62 68 85 108 117 126 166 175 186 202 226	10 20 51 63 91 121 139 162 178 183 184 196	11 31 50 70 89 109 128 148 168 187 206 226	33 47 63 79 96 113 131 149 168 186 203 219	13 31 49 67 86 105 125 144 162 181 201 219	10 26 35 45 50 65 88 113 143 164 196 221	28 39 50 56 73 78 92 101 137 165 186 207	29 47 64 98 108 123 127 141 164 189 211 225

Table 3. *Cont.*

TEST IMAGES	K	TLMVO			LMVO			MVO			ALO			DA			FPA			PSO			CS		
		R	G	B	R	G	B	R	G	B	R	G	B	R	G	B	R	G	B	R	G	B	R	G	B
7	4	64 103 151 225	56 90 158 199	54 127 158 185	64 106 153 221	54 90 158 199	37 72 138 180	64 106 153 221	56 90 158 199	37 72 138 180	64 106 153 221	56 90 158 199	37 72 138 180	64 106 153 225	56 92 167 207	37 72 138 180	80 101 151 229	70 132 177 199	52 90 126 162	64 103 151 225	56 90 158 199	37 72 138 180	73 113 159 226	63 99 151 189	43 68 135 177
	6	58 91 126 161 201 232	54 83 110 149 179 207	36 65 103 134 160 185	44 74 115 153 194 229	45 73 100 144 178 207	34 54 77 122 152 185	58 88 121 154 193 228	43 73 100 144 178 207	36 62 93 130 158 185	58 92 126 161 201 232	54 83 113 149 179 207	36 61 83 127 158 185	58 92 129 162 201 232	54 84 115 149 179 207	34 60 83 127 158 185	58 73 99 130 179 214	30 55 97 133 162 193	25 60 109 134 148 179	58 91 126 161 201 232	45 73 102 144 178 207	36 65 99 130 158 185	53 87 115 151 180 219	43 76 96 131 162 203	32 67 111 146 167 189
	8	44 68 92 120 147 173 205 233	40 65 90 118 149 176 198 219	23 50 73 97 121 142 163 185	44 64 88 116 144 171 204 233	52 74 98 126 154 178 198 219	21 43 70 98 126 152 170 190	44 68 92 121 147 173 205 233	40 63 88 113 142 171 195 219	18 37 56 77 110 136 160 185	44 68 92 121 150 175 205 233	40 63 88 113 144 172 198 219	34 54 73 95 120 142 163 185	44 74 101 129 157 186 212 234	40 61 84 108 141 171 196 219	34 54 77 108 134 158 179 199	31 44 82 106 139 168 192 243	40 61 78 110 137 182 196 211	45 61 110 121 139 165 183 191	44 68 92 121 147 173 205 233	40 63 85 110 14 172 198 219	21 42 62 82 112 136 160 185	42 68 86 109 128 155 176 221	45 54 77 90 127 148 175 207	14 36 68 99 126 155 170 187
	10	44 64 87 107 129 150 171 194 217 235	34 54 73 90 110 133 156 177 198 219	18 34 51 69 85 110 133 156 177 196	41 58 75 97 121 144 166 190 214 234	34 52 69 88 107 132 156 178 198 219	32 49 65 83 107 130 152 170 185 201	44 64 84 103 124 146 169 191 214 234	39 56 74 92 112 136 157 176 198 219	18 36 52 68 85 106 127 147 164 185	44 68 91 115 136 155 175 197 217 236	34 54 74 92 112 134 158 179 199 219	21 37 54 76 98 120 138 156 172 190	44 64 88 112 133 155 178 201 221 238	40 61 83 105 132 156 178 195 208 225	34 54 73 91 110 127 143 160 180 198	35 69 95 115 129 145 166 184 193 229	24 52 73 76 91 105 157 187 199 226	29 40 55 63 120 141 157 162 181 192	44 64 88 108 129 151 173 196 218 238	40 59 79 99 118 139 158 179 199 219	21 37 54 75 100 122 143 163 185 256	54 71 86 104 120 136 152 158 170 227	33 65 98 107 135 143 166 185 197 219	28 62 75 93 118 140 155 166 201 218
	12	32 44 58 74 92 110 129 150 170 192 214 234	34 52 69 84 100 118 138 158 178 194 207 225	18 33 45 61 76 93 110 129 152 169 185 200	32 44 58 74 90 106 126 147 168 190 211 233	29 42 56 69 84 100 118 138 158 179 199 219	18 34 50 64 79 100 120 138 156 170 185 201	41 58 73 88 101 118 134 153 172 193 214 234	31 40 56 73 89 104 124 143 163 180 199 219	21 36 50 65 81 99 116 132 147 161 179 196	44 62 79 99 116 133 151 169 187 204 221 237	34 52 69 84 101 120 140 160 179 195 208 225	21 37 51 65 79 96 114 130 145 160 179 197	44 64 81 98 118 139 159 180 198 214 228 240	34 51 63 79 95 118 141 159 176 190 207 225	21 36 51 66 81 97 116 134 149 165 180 201	37 65 102 108 117 129 141 149 154 177 210 236	43 58 96 119 124 145 161 180 196 207 214 237	18 31 36 41 48 65 74 96 149 175 186 218	44 64 79 97 116 134 152 169 186 204 221 237	34 55 73 90 107 126 144 161 178 195 208 225	18 36 54 72 89 107 124 141 158 172 185 201	24 52 62 79 88 101 114 141 163 186 207 218	26 72 98 114 126 140 158 171 194 204 210 228	13 26 30 40 53 66 92 121 148 163 170 191
8	4	32 80 126 164	29 90 151 223	51 98 146 195	32 80 126 164	47 99 157 223	51 98 146 195	32 78 126 164	47 99 157 223	58 120 181 230	32 80 126 164	47 99 157 223	51 98 146 195	32 78 126 164	47 99 157 223	61 121 181 230	35 78 107 157	87 132 173 232	57 112 185 232	32 80 126 164	47 99 157 223	58 120 181 230	41 89 118 164	40 109 152 224	84 134 187 231
	6	25 56 87 119 150 170	25 68 112 160 204 225	39 78 117 156 196 230	25 56 89 123 150 170	27 71 114 160 207 225	39 76 115 155 195 230	25 57 90 123 150 170	25 59 96 134 174 223	39 78 117 156 195 230	22 51 80 109 135 164	25 60 99 137 176 223	40 79 118 157 196 230	22 51 80 109 135 164	25 68 112 160 207 225	40 79 118 157 196 230	26 85 131 137 163 182	43 94 132 210 226 239	41 102 137 158 193 239	25 58 90 123 150 170	25 60 99 137 176 223	39 78 117 156 196 230	20 36 84 113 148 171	26 52 90 128 204 229	78 114 136 160 197 228
	8	16 39 62 85 109 132 153 170	25 55 85 114 145 176 207 225	28 53 80 107 137 167 199 230	16 39 62 85 109 132 153 170	24 49 74 102 133 166 207 225	29 58 86 115 144 173 202 230	15 36 58 82 106 132 153 170	25 55 85 115 146 177 207 225	29 57 86 115 144 173 202 230	17 40 63 86 109 132 153 170	25 55 86 118 148 178 207 225	31 60 89 118 146 175 203 231	17 38 59 82 106 131 153170	25 55 85 115 147 178 207 225	34 66 98 132 165 198 225 241	35 45 76 91 38 151 164 195	26 64 87 96 149 200 215 237	54 66 104 140 159 194 235 245	17 40 64 87 110 132 153 170	25 55 86 116 148 178 207 225	30 58 86 115 144 173 202 230	17 35 59 98 110 139 158 168	18 54 99 114 129 170 213 235	25 56 81 97 151 183 214 233
	10	15 34 54 74 94 114 134 153 170 187	22 42 62 85 107 129 154 181 207 225	24 46 69 93 118 144 171 199 225 241	16 35 55 75 95 115 135 153 170 182	20 39 58 80 104 129 155 181 207 225	23 45 69 94 118 143 170 199 224 241	14 32 50 68 89 109 129 150 164 181	24 47 72 98 125 153 180 205 223 239	23 44 66 88 112 134 156 179 204 230	13 27 44 61 79 98 117 135 153 170	24 47 70 93 116 140 164 186 207 225	28 53 78 103 128 153 178 202 225 241	15 33 50 67 85 103 119 135 153 170	25 58 84 112 140 167 187 206 223 239	24 46 71 96 121 147 175 202 225 241	5 16 37 57 71 83 109 127 135 162	25 72 79 99 112 145 159 192 208 231	20 27 39 93 128 168 186 214 234 241	16 35 55 75 95 115 135 153 170 256	24 49 75 100 126 153 180 207 223 239	24 46 69 91 114 136 159 182 205 231	31 41 49 64 76 118 130 149 160 175	25 40 58 85 114 149 179 191 207 214	19 56 87 103 111 128 137 160 205 223
	12	13 29 45 61 77 93 109 124 139 155 170 187	24 44 65 85 106 126 146 166 186 207 223 239	21 40 60 80 100 120 140 161 182 204 225 241	13 29 45 63 81 100 118 135 153 170 187 236	20 37 54 73 94 114 135 158 181 204 222 239	19 37 56 75 95 116 137 158 180 202 224 241	13 28 44 61 77 92 108 123 138 153 170 239	20 39 58 79 100 121 142 164 185 205 222 239	18 37 57 76 96 115 136 157 180 203 225 241	13 28 43 58 74 89 104 121 138 155 170 189	24 47 67 86 105 124 143 163 187 207 223 239	23 44 65 85 105 125 143 163 185 205 225 241	16 34 52 71 90 107 123 138 153 170 187 256	22 44 66 88 108 129 149 169 188 207 223 239	25 46 67 86 106 126 148 169 189 207 225 241	12 35 42 49 75 85 103 110 121 127 136 186	7 25 66 107 142 154 168 175 181 200 226 236	45 56 68 76 90 96 121 130 137 170 200 232	13 27 44 60 75 90 105 121 138 153 170 187	22 43 64 85 106 127 148 168 188 207 223 239	21 41 61 81 102 122 143 164 185 205 225 241	16 32 44 54 66 81 89 98 115 129 144 166	51 61 78 97 109 141 156 176 193 209 222 241	34 48 64 94 113 122 126 163 182 195 211 236

Table 3. *Cont.*

TEST IMAGES	K	TLMVO			LMVO			MVO			ALO			DA			FPA			PSO			CS		
		R	G	B	R	G	B	R	G	B	R	G	B	R	G	B	R	G	B	R	G	B	R	G	B
9	4	62 111 164 212	27 86 152 218	44 88 120 154	62 111 164 212	27 86 154 222	44 85 116 154	62 111 163 212	27 86 154 222	48 88 120 154	62 111 164 212	27 86 154 222	48 88 120 154	62 111 164 212	27 86 154 222	48 88 120 154	65 119 154 213	31 72 154 203	54 98 137 180	62 111 164 212	27 86 154 222	44 85 120 154	84 123 170 216	27 70 125 165	48 86 120 162
	6	30 70 107 146 182 219	27 68 106 145 185 222	30 57 85 109 132 158	19 53 91 131 173 219	27 68 106 147 188 227	30 57 85 109 135 167	30 70 107 146 182 219	27 65 100 139 181 222	29 55 82 109 132 158	19 61 99 139 179 219	27 68 106 145 185 222	30 57 85 109 132 158	31 73 111 149 186 219	27 65 101 144 188 227	31 59 85 109 132 161	50 83 142 154 178 227	32 114 127 160 190 217	18 25 55 94 130 184	34 73 111 149 186 219	27 69 109 149 189 227	30 57 85 109 135 167	35 68 110 165 196 217	30 48 79 112 159 198	25 70 92 115 143 162
	8	18 47 77 107 138 168 197 222	27 58 85 112 139 169 199 227	27 48 68 89 109 127 153 178	18 44 73 101 129 159 188 219	21 41 65 93 124 156 191 227	25 48 69 91 111 132 154 178	18 45 75 106 136 166 194 222	22 57 86 115 143 172 204 231	25 45 67 88 109 127 152 178	18 47 77 107 137 167 197 222	22 57 86 115 145 175 206 234	27 48 69 89 110 132 154 178	18 50 82 113 144 172 199 222	22 58 87 116 146 176 206 234	29 52 73 91 109 127 149 172	53 88 123 152 171 203 222 244	25 77 110 147 173 205 227 237	52 69 77 95 103 129 154 171	18 47 77 106 136 166 197 222	22 58 86 115 145 175 206 234	27 48 70 91 109 132 154 178	35 58 91 105 124 150 190 219	29 60 88 122 157 177 185 210	42 67 81 100 122 140 158 180
	10	18 35 53 72 92 114 137 162 190 219	21 38 62 87 112 137 163 189 214 236	25 42 59 77 93 109 126 143 161 178	18 39 61 84 107 131 154 177 201 224	21 36 56 77 100 126 153 181 209 234	20 37 54 71 91 109 126 143 161 178	18 37 56 77 96 119 142 167 193 219	21 39 63 86 109 133 159 185 210 234	24 41 58 73 91 109 126 153 178 225	18 40 63 87 110 132 155 179 202 224	21 40 65 88 113 139 163 187 210 234	25 42 59 75 91 109 125 140 158 178	18 43 66 89 113 138 164 193 219 243	22 51 76 101 128 152 176 198 219 238	24 40 56 73 91 109 126 143 161 178	57 81 99 127 146 169 189 194 213 237	31 55 94 118 145 167 187 193 208 230	16 29 55 65 91 95 123 145 166 195	18 41 67 92 118 143 169 194 219 243	21 41 65 90 116 142 168 194 218 238	24 40 59 77 92 109 126 143 161 178	31 63 85 94 109 121 163 184 210 224	24 53 72 108 135 147 164 178 208 240	41 58 76 104 128 140 149 161 173 179
	12	18 35 55 75 95 115 135 155 176 197 219 240	21 35 53 71 90 109 128 148 169 191 214 236	20 37 54 72 89 106 120 132 144 156 169 182	18 35 54 74 94 115 136 157 178 199 219 243	9 21 38 61 82 102 124 146 169 191 214 236	19 32 47 61 77 92 107 120 134 149 166 182	18 33 50 68 87 105 127 148 169 190 212 230	21 36 55 74 95 114 134 153 174 195 218 236	14 25 37 51 65 79 94 109 125 143 161 178	18 40 59 77 96 117 138 157 176 197 219 243	21 37 58 77 98 119 141 161 181 201 222 238	20 35 51 66 82 97 112 127 145 162 178 244	18 40 61 81 99 118 136 153 177 201 222 243	21 41 65 88 109 129 150 170 189 208 226 242	16 30 45 61 77 91 106 120 135 153 169 182	20 63 72 89 125 140 148 152 165 193 208 234	25 77 100 119 125 152 166 177 193 218 240 249	12 19 59 93 105 117 129 137 154 165 175 209	18 40 61 82 102 124 145 166 186 206 224 243	21 37 58 77 97 118 138 159 180 201 222 238	16 29 43 57 71 85 97 111 127 146 162 178	38 74 91 106 136 162 174 182 205 212 224 230	31 44 69 80 89 115 133 166 174 188 212 238	32 62 78 95 110 125 137 147 157 166 175 185
10	4	11 55 155 202	27 92 158 215	52 96 147 196	11 54 143 202	27 92 158 215	52 96 147 196	11 55 155 202	27 92 158 215	52 96 147 196	38 100 155 202	52 100 158 215	52 96 147 196	11 54 143 202	27 92 158 215	52 96 147 196	43 86 135 197	57 111 160 206	39 97 170 199	11 55 155 202	27 92 158 215	52 96 147 196	44 105 161 200	39 90 145 220	65 111 144 192
	6	9 45 90 131 168 208	24 54 90 129 168 215	22 53 88 125 161 199	9 43 88 130 168 207	26 67 106 146 180 217	49 83 117 150 182 212	9 44 88 130 168 208	26 67 104 144 179 217	22 53 90 129 168 202	10 47 90 131 168 208	24 54 92 132 171 217	22 53 88 127 166 202	10 47 90 132 169 212	24 55 94 140 180 217	22 53 90 129 168 202	26 67 115 156 192 244	15 43 74 115 167 213	40 71 85 131 174 212	10 47 90 131 168 208	26 67 106 146 180 217	22 53 90 129 168 202	4 41 96 141 176 214	25 99 119 154 199 225	23 59 95 133 185 213
	8	9 41 70 102 135 166 196 224	24 52 77 104 132 160 189 220	22 51 81 108 134 161 188 216	8 35 59 85 114 143 172 212	24 52 79 107 137 165 192 220	22 51 81 108 136 164 193 221	9 40 66 94 124 155 189 219	24 52 77 104 131 159 187 220	22 52 82 111 140 169 197 223	9 41 70 101 133 162 193 221	24 52 78 106 134 161 190 220	22 52 83 112 142 170 199 224	9 41 69 99 130 162 194 224	24 54 89 122 153 184 214 234	22 53 86 121 155 186 214 244	29 52 78 99 116 150 208 226	26 54 106 150 178 222 238 249	22 34 62 87 126 167 177 199	9 41 69 99 131 162 194 224	24 52 77 104 132 160 189 220	22 52 83 112 140 169 197 223	10 61 98 116 132 164 182 221	25 75 95 117 152 166 207 225	48 66 94 131 168 196 215 227
	10	9 39 63 90 116 141 166 189 211 232	20 36 53 73 95 118 141 165 190 220	18 39 59 82 105 128 152 177 202 226	8 29 50 73 96 121 145 169 196 222	23 45 65 84 103 124 147 171 196 221	18 43 63 87 108 129 152 175 199 224	9 38 58 83 107 131 155 177 202 224	23 49 72 96 120 144 166 190 214 233	18 43 64 88 110 132 154 177 202 225	9 39 62 85 108 132 155 178 202 228	24 50 73 96 120 144 166 190 214 234	19 46 67 88 110 135 157 180 202 226	9 40 67 93 119 145 169 196 219 238	23 46 67 91 115 139 163 189 214 234	18 46 68 91 118 145 175 204 226 244	9 20 43 112 146 174 193 212 239 252	31 47 49 64 91 114 139 156 205 227	20 34 75 97 111 134 170 177 205 223	9 38 61 86 108 132 155 177 202 228	24 50 73 96 120 144 167 190 214 234	22 49 75 99 125 150 175 199 223 244	4 32 49 76 99 124 143 181 207 221	23 41 65 86 105 144 174 179 212 227	18 63 87 119 143 158 180 209 229 244
	12	7 27 47 69 90 111 132 153 172 192 212 232	23 42 60 78 97 117 137 156 175 194 214 233	17 34 52 70 88 107 125 144 162 182 202 226	7 23 41 58 76 94 114 134 155 176 202 225	23 42 60 79 98 117 137 156 175 194 214 234	18 38 58 80 99 120 140 161 182 202 223 244	7 24 41 60 81 101 120 138 156 177 202 228	20 36 53 71 89 109 127 147 168 190 213 232	16 32 49 66 83 101 123 144 165 185 204 227	8 28 49 71 90 111 133 155 176 196 216 238	22 39 56 76 96 116 136 156 175 194 214 233	18 36 53 73 91 110 129 149 169 188 207 228	7 23 45 65 90 113 131 153 174 196 215 238	24 48 69 91 112 131 150 170 189 208 223 239	19 44 65 87 108 128 149 170 191 209 228 244	17 47 79 101 113 146 152 173 191 221 233 253	21 37 58 79 97 119 133 155 172 192 222 232	26 49 64 88 101 110 134 146 167 178 196 238	8 28 49 69 90 113 134 155 174 196 216 238	21 38 54 73 94 114 134 153 172 193 214 234	18 38 58 80 100 121 142 163 184 204 226 244	21 55 93 105 120 130 142 169 186 202 209 237	23 31 52 61 82 109 133 146 175 194 205 232	23 27 42 59 73 90 120 144 162 181 202 224

5.3. Performance Metric

We performed the experimental from both Performance evaluation and Statistical evaluation. The methods used are shown in Table 4.

Table 4. The definition and description of performance measures.

Category	Name	Formulation	Remark	Reference
Performance evaluation	Structural Similarity Index	$SSIM(I,\hat{I}) = \frac{(2\mu_I\mu_{\hat{I}}+c_1)(2\sigma_I\sigma_{\hat{I}}+c_2)}{(\mu_I^2+\mu_{\hat{I}}^2+c_1)(\sigma_I^2+\sigma_{\hat{I}}^2+c_2)}$	The index that measures the similarity between the two images before and after the segmentation, the closer the value is to 1, the better the image segmentation effect.	[64]
	Feature Similarity Index	$FSIM = \frac{\sum_{x\hat{I}\Omega} S_L(x)\times PC_m(x)}{\sum_{x\hat{I}\Omega} PC_m(x)}$	An indicator for evaluating the local structural importance between the original image and the segmented image, the maximum value is 1.	[65]
	Peak Signal to Noise Ratio	$PSNR = 20log(\frac{255}{RMSE})(dB)$	Represents the ratio between the maximum possible power of a signal and the power of corrupting noise. The larger the value, the better the effect. It is not absolutely proportional to the observation of the human eye, and has some limitations.	[66]
	Root Mean Squared Error	$RMSE = \sqrt{\left(\sum_{i=1}^{M}\sum_{j=1}^{N}(I(i,j)-\hat{I}(i,j))^2\right)/(M\times N)}$	Computes the difference between the predicted value. In general, it is directly used in PSNR. As can be seen from the formula, it is inversely proportional to PSNR.	[67]
	Mean Operating Time	$Time = \frac{\sum_{i=1}^{N} time}{N}$	The computational complexity is evaluated by experimental data. Average the execution time of each algorithm running independently for 30 times. The smaller the numerical value, the faster the algorithm is executed and the lower the computational complexity.	[68]
	Average fitness function value	$Fitness = \frac{\sum_{i=1}^{N} f_i}{N}$	The mathematical concept of optimization is the method of calculating the value of a function and finding the optimal result by maximizing and minimizing an objective function in a given domain. Therefore, the average fitness value obtained through multiple measurements can be used to evaluate the optimization results.	[69]
Statistical evaluation	Wilcoxon's Rank-Sum test	$R^+ = \sum_{d_i>0} rank(d_i) + \frac{1}{1}\sum_{d_i=0} rank(d_i)$ $R^- = \sum_{d_i<0} rank(d_i) + \frac{1}{2}\sum_{d_i=0} rank(d_i)$	Used to answer the question "Does two samples represent two different populations?" In this paper, it is used to compare the difference between the proposed algorithm and the comparison algorithm. If the p-value > 0.05 (or h = 1), there is a significant difference, otherwise it is not.	[70]
	Friedman test	$F_f = \frac{12n}{k(k+1)}\left[\sum_j R_j^2 - \frac{k[k+1]^2}{4}\right]$	The Friedman test is a nonparametric simulation of nonparametric variance bidirectional analysis. Used to answer the question "Does at least two samples in a group of k samples represent populations with different median values?" Designed to detect significant differences between the behavior of two or more algorithms, the overall performance of the algorithm can be ranked.	[70]

5.4. Implementation Results and Discussion

In this section, the experimental results of the TLMVO-Masi multilevel threshold are described and analyzed in detail. According to the above metrics, it is analyzed from three aspects: image performance indicators, segmentation function performance index and mathematical statistics of data results. The superiority of TLMVO algorithm over other effective algorithms is verified. The following is a sub-section discussion.

5.4.1. Image Segmentation Quality

Measuring the performance by intensity and accuracy, Structural Similarity Index (SSIM), Feature Similarity Index (FSIM), and Peak Signal to Noise Ratio (PSNR) are ultilized. Segmentation effects of 10 satellite images are shown in Figure 6. Different thresholds of different algorithms of an image run 30 times, and then correspond to three indexes. The overall data space size is $3 \times 10 \times 8 \times 5 = 1200$ (10 images, 8 algorithms, 5 thresholds). Average data results of 30 times are indicated in Tables 5–7, respectively. The higher the similarity between the original image and the segmented image, the greater the value (the maximum value of SSIM and FSIM is 1). The maximum value of the index corresponding to each threshold is indicated by a distinct mark in tables.

These three tables clearly show that, as the threshold value increases, the value of the indicator also increases. This indicates that the segmentation quality is improved with the increase of threshold number, which can also correspond to the segmentation renderings we have given. As the threshold value increases, the segmentation image becomes clearer.

From the label distribution, it can be seen that most of the three index values of the proposed algorithm are more outstanding than comparison algorithms. For instance, in the case of various thresholds of TLMVO:

1. In the SSIM table: the values of Image 1 and Image 3 are all higher than the comparison algorithm;
2. In the FSIM table: Image 3 and Image 6 yield excellence values compared with other algorithms in all cases;
3. In the PSNR table: the values in Image 1, Image 3, and Image 8 are all much better than the comparative algorithms.

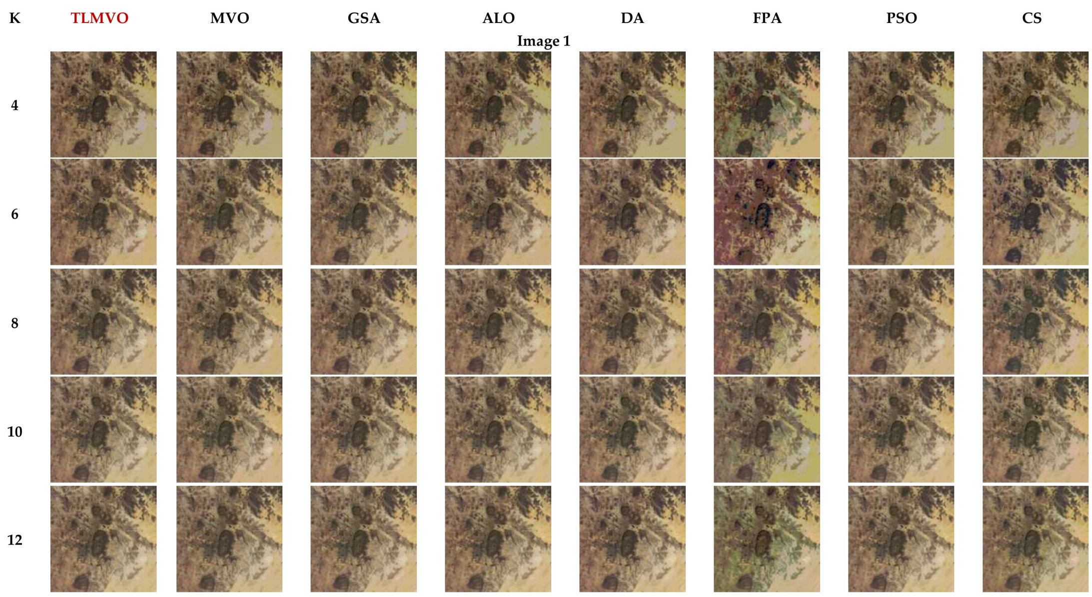

Figure 6. *Cont.*

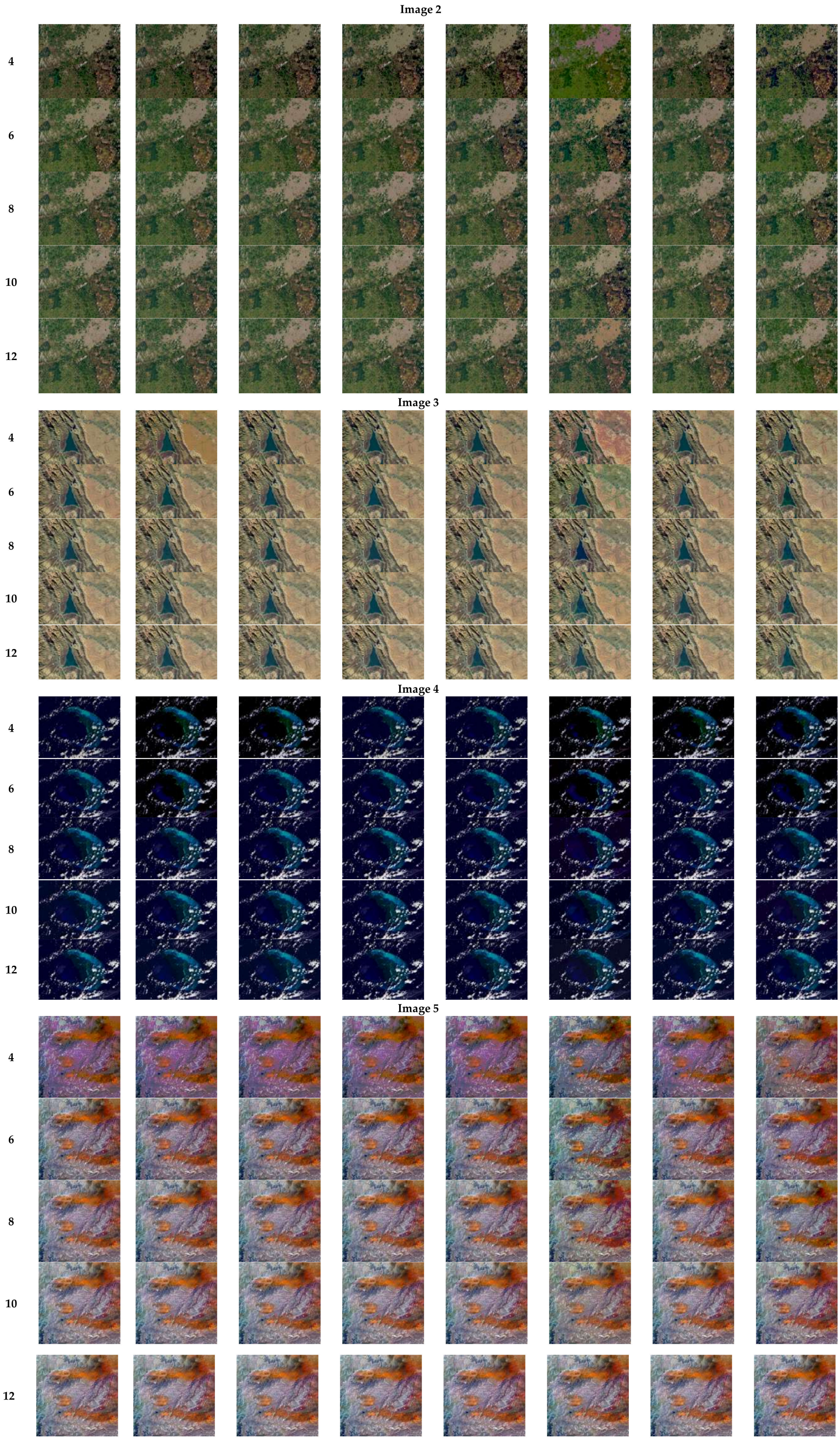

Figure 6. *Cont.*

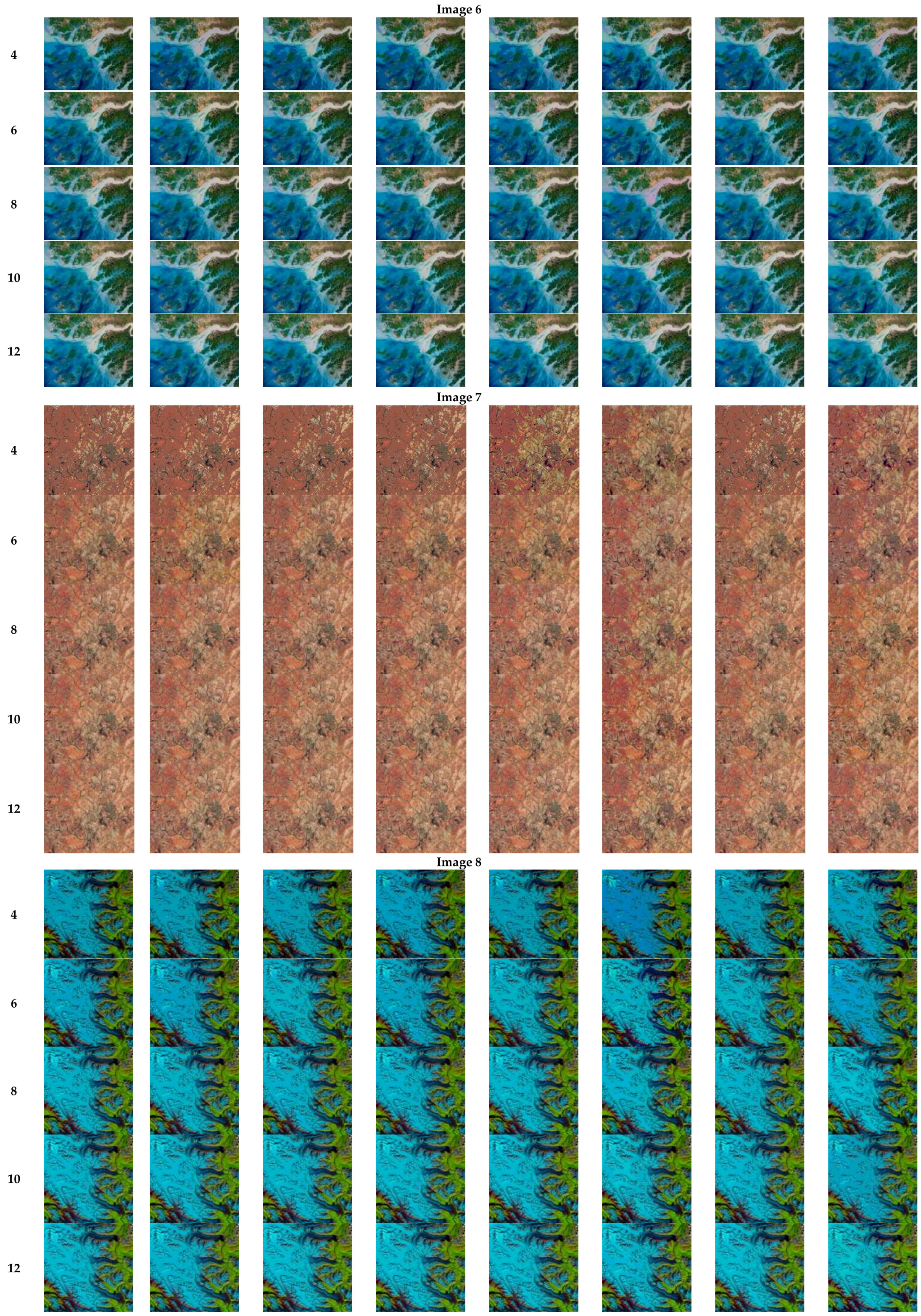

Figure 6. *Cont.*

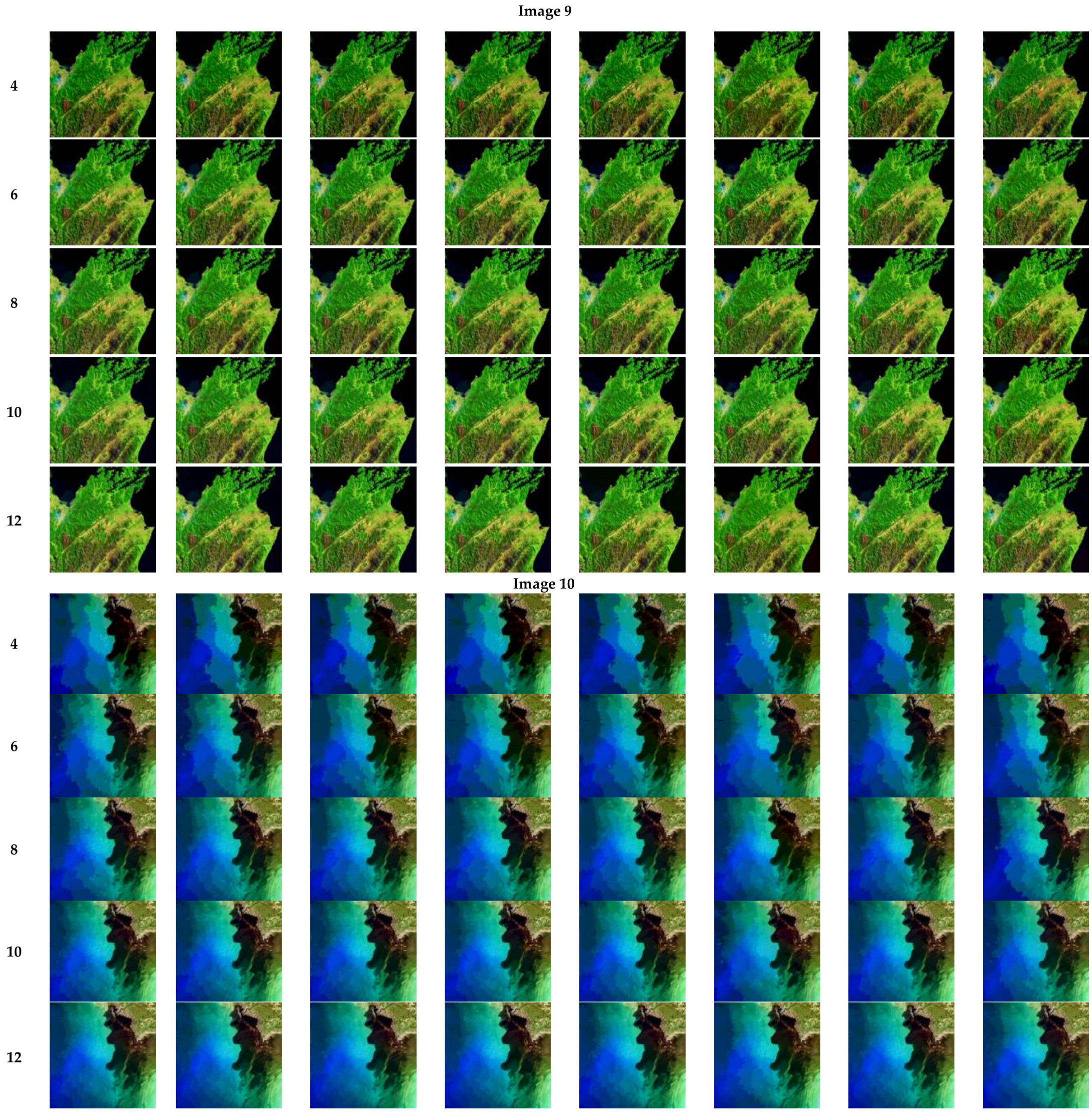

Figure 6. Segmentation renderings of 10 satellite images.

In order to more clearly see the superiority of TLMVO, the three index values of each test image are integrated into three line graphs (as shown in Figures 7–9). The data of TLMVO algorithm are represented in green. The green line can include other colored lines. To some extent, the results confirm that the improved algorithm can achieve good image segmentation quality.

Table 5. The SSIM of each algorithm under Masi entropy.

TEST IMAGES	K	TLMVO	LMVO	MVO	ALO	DA	FPA	PSO	CS
1	4	0.7744	0.7715	0.7740	0.7715	0.7723	0.7502	0.7715	0.7512
	6	0.8566	0.8559	0.8558	0.8467	0.8556	0.7868	0.8408	0.8337
	8	0.8994	0.8965	0.8862	0.8984	0.8923	0.8279	0.8971	0.8819
	10	0.9296	0.9291	0.9239	0.9293	0.9278	0.8780	0.9262	0.8645
	12	0.9438	0.9423	0.9413	0.9435	0.9393	0.8903	0.9383	0.9115
2	4	0.7122	0.6452	0.6872	0.6855	0.6909	0.6702	0.6150	0.6914
	6	0.8349	0.8151	0.8535	0.8542	0.8477	0.7471	0.8299	0.7989
	8	0.9135	0.8964	0.8888	0.9052	0.8895	0.8649	0.8903	0.8605
	10	0.9408	0.9317	0.9259	0.9271	0.9257	0.8708	0.9357	0.8901
	12	0.9547	0.9489	0.9468	0.9528	0.9519	0.9070	0.9443	0.9265
3	4	0.7959	0.7898	0.7830	0.7897	0.7914	0.7027	0.7502	0.7826
	6	0.8726	0.8714	0.8694	0.8590	0.8650	0.8523	0.8654	0.8605
	8	0.9133	0.9093	0.9085	0.9126	0.9101	0.8881	0.9091	0.8827
	10	0.9415	0.9383	0.9386	0.9399	0.9404	0.8944	0.9383	0.9236
	12	0.9580	0.9533	0.9537	0.9552	0.9529	0.9128	0.9569	0.9359
4	4	0.4083	0.3809	0.3809	0.3762	0.3805	0.3674	0.3762	0.3791
	6	0.6019	0.6002	0.5926	0.5929	0.5910	0.5836	0.5919	0.4427
	8	0.6364	0.6362	0.6364	0.6195	0.6120	0.5571	0.6169	0.5880
	10	0.7692	0.6526	0.6575	0.6532	0.6446	0.7614	0.7666	0.6435
	12	0.7736	0.6744	0.6741	0.6649	0.6616	0.6895	0.7734	0.6183
5	4	0.6682	0.6681	0.6239	0.6429	0.6271	0.6573	0.6430	0.6239
	6	0.8053	0.8133	0.8022	0.8142	0.8074	0.7861	0.8034	0.7772
	8	0.8819	0.8804	0.8786	0.8734	0.8739	0.8024	0.8789	0.8362
	10	0.9142	0.9120	0.9115	0.9138	0.9104	0.8940	0.9119	0.8937
	12	0.9420	0.9375	0.9348	0.9407	0.9416	0.8578	0.9402	0.9046
6	4	0.7156	0.7156	0.7138	0.7138	0.7115	0.6512	0.7138	0.6914
	6	0.8033	0.8084	0.8046	0.8032	0.8018	0.7928	0.8030	0.8075
	8	0.8562	0.8548	0.8551	0.8550	0.8551	0.7803	0.8541	0.8022
	10	0.8862	0.8847	0.8830	0.8802	0.8674	0.8332	0.8844	0.8738
	12	0.9050	0.9007	0.8971	0.9037	0.8975	0.8567	0.9007	0.8661
7	4	0.5752	0.6157	0.6152	0.6152	0.5965	0.5903	0.6046	0.5536
	6	0.8252	0.7880	0.8201	0.8200	0.8244	0.7817	0.8250	0.8182
	8	0.8907	0.8825	0.8756	0.8968	0.8775	0.8091	0.8789	0.8479
	10	0.9294	0.9284	0.9185	0.9258	0.9228	0.7486	0.9249	0.8523
	12	0.9507	0.9492	0.9449	0.9491	0.9412	0.8673	0.9502	0.9157
8	4	0.6910	0.6999	0.6811	0.6999	0.6794	0.6687	0.6805	0.6399
	6	0.7761	0.7766	0.7896	0.8021	0.7871	0.6895	0.7892	0.7106
	8	0.8648	0.8616	0.8555	0.8565	0.8507	0.7228	0.8574	0.8287
	10	0.8961	0.8959	0.8930	0.8952	0.8885	0.8764	0.8854	0.8154
	12	0.9159	0.9126	0.9121	0.9104	0.8967	0.8502	0.9139	0.8714
9	4	0.5578	0.5576	0.5435	0.5434	0.5434	0.5077	0.5575	0.5120
	6	0.7024	0.7047	0.7059	0.6993	0.6940	0.7032	0.7016	0.6858
	8	0.7578	0.7555	0.7470	0.7484	0.7380	0.6107	0.7480	0.6813
	10	0.7967	0.7780	0.7825	0.7762	0.7789	0.7741	0.7771	0.6913
	12	0.8625	0.8042	0.8506	0.8063	0.8382	0.7635	0.8393	0.7152
10	4	0.6274	0.6237	0.6237	0.5968	0.6238	0.5912	0.6237	0.5927
	6	0.7429	0.7001	0.7331	0.7412	0.7360	0.6911	0.7316	0.7057
	8	0.7779	0.7829	0.7777	0.7757	0.7614	0.7353	0.7764	0.6985
	10	0.8147	0.8143	0.8005	0.7991	0.7917	0.7798	0.7958	0.7905
	12	0.8439	0.8406	0.8434	0.8361	0.8315	0.7940	0.8328	0.7981

Table 6. The FSIM of each algorithm under Masi entropy.

TEST IMAGES	K	TLMVO	LMVO	MVO	ALO	DA	FPA	PSO	CS
1	4	0.8408	0.8401	0.8379	0.8379	0.8389	0.8138	0.8379	0.8199
	6	0.9109	0.9093	0.8870	0.9039	0.9089	0.8440	0.8990	0.8856
	8	0.9332	0.9395	0.9416	0.9410	0.9352	0.8850	0.9405	0.9193
	10	0.9572	0.9514	0.9607	0.9616	0.9599	0.9209	0.9597	0.9079
	12	0.9697	0.9695	0.9671	0.9690	0.9684	0.9279	0.9672	0.9396
2	4	0.8433	0.8398	0.8214	0.8279	0.8338	0.8218	0.7855	0.8108
	6	0.9157	0.9055	0.9321	0.9331	0.9223	0.8618	0.9158	0.9019
	8	0.9592	0.9534	0.9490	0.9556	0.9482	0.9216	0.9501	0.9306
	10	0.9736	0.9692	0.9662	0.9672	0.9660	0.9298	0.9717	0.9369
	12	0.9803	0.9735	0.9776	0.9791	0.9786	0.9433	0.9752	0.9570
3	4	0.8967	0.8941	0.8935	0.8679	0.8962	0.8358	0.8723	0.8842
	6	0.9447	0.9398	0.9439	0.9390	0.9398	0.9188	0.9420	0.9269
	8	0.9641	0.9625	0.9587	0.9615	0.9605	0.9393	0.9610	0.9380
	10	0.9751	0.9743	0.9743	0.9746	0.9741	0.9513	0.9738	0.9581
	12	0.9816	0.9804	0.9801	0.9806	0.9799	0.9528	0.9812	0.9682
4	4	0.8717	0.8640	0.8640	0.8630	0.8650	0.8492	0.8630	0.8595
	6	0.8928	0.9137	0.9124	0.9130	0.9123	0.8932	0.9123	0.9062
	8	0.9337	0.9335	0.9335	0.9312	0.9301	0.8839	0.9308	0.9115
	10	0.9496	0.9453	0.9435	0.9452	0.9377	0.9219	0.9488	0.9255
	12	0.9558	0.9536	0.9541	0.9533	0.9512	0.9200	0.9540	0.9299
5	4	0.7343	0.7729	0.7343	0.7543	0.7427	0.7661	0.7540	0.7724
	6	0.8878	0.8874	0.8805	0.8809	0.8817	0.8570	0.8807	0.8546
	8	0.9335	0.9335	0.9347	0.9314	0.9302	0.8667	0.9332	0.8994
	10	0.9552	0.9540	0.9537	0.9544	0.9515	0.9316	0.9536	0.9294
	12	0.9703	0.9676	0.9668	0.9651	0.9695	0.9023	0.9694	0.9421
6	4	0.8092	0.8092	0.8081	0.8081	0.8062	0.7641	0.8081	0.7926
	6	0.8807	0.8754	0.8794	0.8794	0.8793	0.8494	0.8792	0.8724
	8	0.9232	0.9171	0.9218	0.9219	0.9223	0.8545	0.9207	0.8690
	10	0.9442	0.9438	0.9279	0.9415	0.9357	0.8981	0.9353	0.9289
	12	0.9555	0.9545	0.9539	0.9551	0.9526	0.9145	0.9541	0.9186
7	4	0.7974	0.7376	0.7369	0.7369	0.7212	0.7106	0.7284	0.7651
	6	0.9064	0.8779	0.8985	0.8983	0.9014	0.8786	0.9053	0.8959
	8	0.9495	0.9423	0.9379	0.9471	0.9402	0.8763	0.9399	0.9125
	10	0.9646	0.9632	0.9685	0.9685	0.9671	0.8356	0.9667	0.9082
	12	0.9785	0.9764	0.9756	0.9780	0.9743	0.9076	0.9736	0.9528
8	4	0.8378	0.8395	0.8243	0.8395	0.8230	0.8101	0.8246	0.7957
	6	0.8914	0.8904	0.9010	0.9078	0.8962	0.8173	0.9014	0.8249
	8	0.9400	0.9360	0.9396	0.9385	0.9347	0.8508	0.9391	0.9090
	10	0.9584	0.9554	0.9562	0.9582	0.9546	0.9211	0.9538	0.9145
	12	0.9686	0.9675	0.9666	0.9662	0.9632	0.9262	0.9681	0.9396
9	4	0.8541	0.8534	0.8473	0.8472	0.8472	0.8278	0.8534	0.8221
	6	0.9285	0.9276	0.9283	0.9277	0.9249	0.8928	0.9274	0.9081
	8	0.9502	0.9487	0.9487	0.9485	0.9466	0.8913	0.9482	0.9213
	10	0.9585	0.9618	0.9588	0.9590	0.9580	0.9402	0.9575	0.9241
	12	0.9747	0.9709	0.9658	0.9666	0.9708	0.9292	0.9715	0.9377
10	4	0.7640	0.7640	0.7599	0.7634	0.7640	0.7528	0.7599	0.7514
	6	0.8242	0.8210	0.8240	0.8250	0.8226	0.8073	0.8244	0.8015
	8	0.8620	0.8598	0.8596	0.8592	0.8478	0.8242	0.8592	0.8300
	10	0.8917	0.8837	0.8834	0.8829	0.8762	0.8494	0.8810	0.8619
	12	0.9113	0.9092	0.9108	0.9084	0.9036	0.8819	0.9059	0.8802

Table 7. The PSNR of each algorithm under Masi entropy.

TEST IMAGES	K	TLMVO	LMVO	MVO	ALO	DA	FPA	PSO	CS
1	4	20.7925	20.7725	20.7675	20.7125	20.7915	20.2532	20.7125	20.1630
	6	24.1576	23.4460	24.1240	23.7732	24.1316	20.8999	22.9504	22.8607
	8	26.2592	26.0185	25.5235	26.2024	25.9712	23.5785	26.1342	25.3450
	10	28.3717	28.1962	28.1737	28.2740	28.2269	25.6046	28.0548	24.8368
	12	29.6100	29.3884	29.3109	29.6050	29.2210	26.4913	29.0708	27.2000
2	4	18.8430	18.8249	18.6134	18.9307	18.9290	18.2521	17.2951	18.1679
	6	22.3266	21.6960	22.8578	22.8863	22.5439	20.4732	22.1872	21.1393
	8	24.2476	24.6675	25.3874	24.9641	24.3533	23.5434	24.3869	23.5563
	10	27.2892	27.2621	27.2874	26.3446	26.2204	24.1414	26.8406	24.8671
	12	28.5535	27.9996	27.9939	28.3447	28.3496	25.8873	27.6342	26.8304
3	4	19.9262	18.8001	19.6044	18.8017	19.8648	17.8319	18.9799	19.5485
	6	22.6252	22.3173	22.5656	22.2449	22.6239	21.8502	22.4853	22.4241
	8	24.7823	24.5854	24.5670	24.7439	24.3765	23.6344	24.2951	23.1364
	10	26.4116	26.3248	26.3246	26.4026	26.3820	24.7313	25.5045	25.7397
	12	28.2060	27.6567	27.8359	27.8759	27.7598	25.1138	28.0180	26.7576
4	4	21.7947	19.5676	19.5676	19.5394	19.5675	19.2235	19.5394	19.5386
	6	21.0832	23.8521	23.7218	23.7330	23.6856	22.5114	23.7101	23.4854
	8	25.0875	25.0789	25.0852	24.8347	24.7279	23.2739	24.8134	23.3235
	10	27.1861	26.1187	25.9677	26.1052	25.4995	25.7035	27.0715	25.3684
	12	27.4950	26.9966	26.9420	26.9006	26.5768	25.5771	26.7394	24.9418
5	4	16.9806	17.8866	16.9806	17.4367	16.8512	17.2823	17.4483	17.8100
	6	21.3662	21.1859	20.9164	21.2681	21.0219	20.6315	20.9578	20.5071
	8	23.5702	23.6344	23.6781	23.4792	23.3843	21.1273	23.5965	22.0975
	10	25.3535	25.3249	25.3250	25.3295	25.1868	24.7880	25.2063	24.7622
	12	26.2153	26.9166	26.6882	27.1381	27.3483	23.7282	27.1303	25.8037
6	4	20.5027	20.5027	20.4732	20.4732	20.4333	19.0972	20.4732	19.9978
	6	23.4533	23.4390	23.4334	23.4054	23.4079	21.9773	23.3958	23.1176
	8	25.9008	25.8499	25.8486	25.8400	25.8486	22.5025	25.7739	23.2438
	10	26.9624	26.5210	27.5186	27.2226	26.6858	24.7022	27.4974	26.6856
	12	28.4770	28.5111	28.4938	28.5166	28.1274	25.8854	28.3971	26.2981
7	4	17.3110	17.3778	17.3814	17.3814	17.1450	17.2728	17.1777	17.2192
	6	22.1716	21.8913	21.8272	22.0566	21.9270	20.5434	21.9065	21.8887
	8	24.8042	24.0714	23.9957	24.7965	23.9964	21.9582	24.1262	23.0275
	10	26.6863	26.3535	26.0397	26.6338	26.4948	21.6290	26.4367	24.1686
	12	28.3561	28.3134	27.9492	28.3138	27.6726	24.4441	27.6680	26.2470
8	4	20.0461	20.0461	19.4775	20.0461	19.4719	19.5537	19.4627	19.0435
	6	23.2358	22.7455	22.7302	23.0977	22.4261	19.4761	22.7791	19.9978
	8	25.2157	25.1023	24.7838	25.2140	24.9005	21.5724	25.1973	23.3424
	10	27.3115	26.7463	26.7323	27.2165	26.7850	25.1312	26.6258	24.5564
	12	28.4387	28.3717	28.2705	28.3854	28.0137	25.4779	28.4350	27.1038
9	4	19.2111	19.1843	19.0203	19.0148	19.0148	18.4891	19.1816	18.8663
	6	22.8662	22.7671	22.8598	22.6730	22.5579	21.6290	22.7617	22.0944
	8	24.6355	24.6272	24.7685	24.5523	24.3009	21.5557	24.5443	23.4442
	10	26.1033	26.3495	26.2421	26.0171	25.9568	24.6928	25.7938	23.8834
	12	28.1868	27.7538	27.5842	27.2778	27.9255	24.1660	27.0234	24.3194
10	4	18.5418	18.8095	18.5418	19.9601	18.8095	19.7825	18.5418	19.6373
	6	22.9894	22.6055	22.8154	22.9843	22.8644	22.2684	22.8347	21.0550
	8	25.2811	25.5629	25.3434	25.2261	24.4932	23.5053	25.2552	22.7493
	10	27.3663	27.3658	26.7641	26.7074	26.1830	24.0665	26.5807	25.4793
	12	28.8324	28.6704	28.6576	28.6044	28.0206	27.0101	28.3926	27.1410

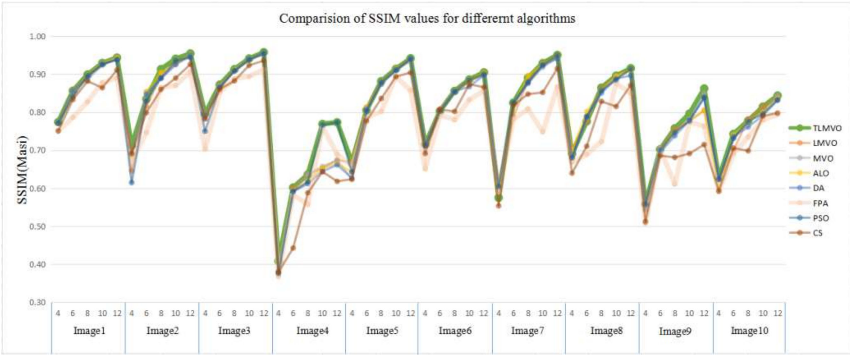

Figure 7. Broken line chart of SSIM indicator.

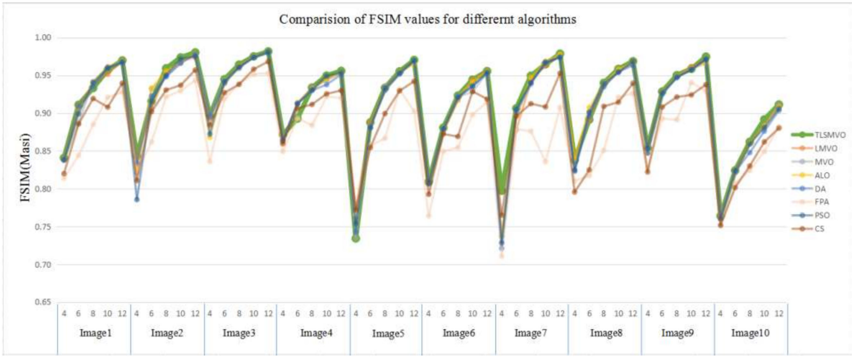

Figure 8. Broken line chart of FSIM indicator.

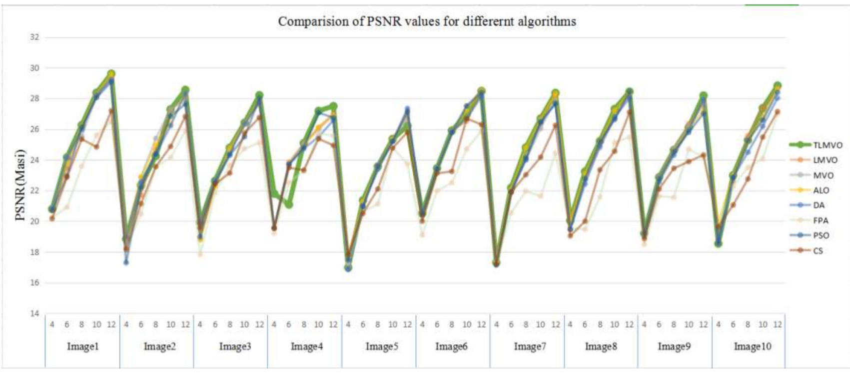

Figure 9. Broken line chart of FSIM indicator.

5.4.2. Fitness Function Value Analysis

A Masi entropy couple with an optimization algorithm to image segmentation is to take Masi entropy function as the fitness function of optimization. Therefore, the fitness function value can be a major concern to evaluate the performance of algorithm.

Table 8 is the average value of the fitness function values obtained by the TLMVO-Masi method for 30 times, wherein the maximum value of fitness functions corresponding to various threshold values are expressed by adding shadows. Under the condition of the maximum threshold, the convergence curves of the TLMVO algorithm compared with other algorithms are shown in Figure 10, which is mainly used for the analysis of convergence speed and robustness. The convergence curve of TLMVO is marked in red for distinction. In order to make a visual observation, furthermore, box plots corresponding to each set of convergence curves are produced to consolidate the judgment on the stability of the algorithm.

Table 8. The optimal fitness value of each algorithm under Masi entropy.

TEST IMAGES	K	TLMVO	LMVO	MVO	ALO	DA	FPA	PSO	CS
1	4	26.7841	26.7829	26.7759	26.7829	26.7814	26.5055	26.7829	26.5970
	6	31.5270	32.3884	32.4733	32.4287	32.4701	30.8250	32.4650	31.7859
	8	37.4559	37.4196	37.4012	37.4534	37.3572	34.7005	36.4051	36.3904
	10	41.7545	40.3203	41.6523	41.7150	41.6303	37.9999	41.5054	39.5423
	12	45.4460	45.4398	45.2587	45.4081	45.4063	42.1282	44.2942	42.7526
2	4	28.6708	28.6708	28.6708	28.6395	28.6330	27.8866	28.6523	28.3837
	6	34.8390	34.7560	34.8757	34.8782	34.8344	33.5580	34.8406	34.3164
	8	40.2542	40.1957	40.1659	40.2540	40.2045	38.0999	40.2133	39.6369
	10	45.0650	45.0265	44.9409	45.0126	44.8228	42.3067	44.8578	43.0264
	12	49.1601	49.0709	48.9234	49.1108	49.0990	45.7133	48.5453	46.3682
3	4	29.7577	29.7323	29.7778	29.7830	29.7760	29.4473	29.7831	29.6724
	6	36.0540	36.0462	36.0337	36.0490	36.0312	35.1721	36.0420	35.4629
	8	41.4123	41.4249	41.4764	41.4795	41.4817	40.0575	41.4816	40.2871
	10	46.3981	46.3759	46.3513	46.3908	46.3270	43.8415	46.3492	44.9901
	12	50.6654	50.6416	50.5188	50.0293	50.6070	48.5678	50.6194	48.8457
4	4	31.8638	31.8631	31.8631	31.8638	31.8628	31.5520	31.8638	31.7064
	6	38.4658	38.4457	38.3229	38.4712	38.4541	37.6742	38.4701	38.0972
	8	44.1409	44.1299	44.1215	44.1379	44.1130	41.8809	44.1281	43.0865
	10	49.1757	49.1380	49.0402	49.1403	48.9261	46.7316	49.0453	47.3696
	12	53.6061	53.5976	53.5837	53.5429	53.4373	50.2012	52.8905	51.2963
5	4	31.2635	31.2635	31.2635	31.2674	31.2400	30.9963	31.2667	31.0917
	6	38.0624	38.0590	38.0595	38.0481	38.0599	37.0511	38.0598	37.6129
	8	43.9486	43.9541	43.9283	43.9474	43.9390	42.3299	43.9476	43.0948
	10	49.0856	49.0812	49.0386	49.0735	49.0009	46.9090	48.9981	46.9546
	12	53.6589	53.6476	53.5966	53.6480	53.5644	51.3290	53.4092	51.4370
6	4	30.1881	30.1881	30.1884	30.1884	30.1868	29.8118	30.1884	30.0943
	6	36.3190	36.3116	36.3166	36.3189	36.3107	35.2884	36.3189	35.7087
	8	41.5411	41.5357	41.4566	41.5381	41.5376	39.0273	41.5191	40.3121
	10	46.1437	46.1336	45.8943	46.1245	46.0484	44.1846	46.1421	45.1448
	12	50.4025	50.3495	49.7042	50.4011	50.3494	46.8572	50.0727	47.8994
7	4	28.2182	28.3445	28.3453	28.3453	28.3106	27.5565	28.3456	28.0657
	6	35.0028	34.9839	34.9229	34.9842	34.9778	33.8109	34.9850	34.4786
	8	40.6323	40.4641	40.6104	40.5998	40.5242	38.6748	40.6264	39.6272
	10	45.4981	45.4799	45.4692	45.4722	45.3232	42.7771	44.7652	43.0443
	12	49.7507	49.5460	49.5312	49.7327	49.6270	45.9063	49.4327	46.5936
8	4	30.6144	30.6455	30.6434	30.6355	30.6434	30.0874	30.6435	30.4565
	6	37.0419	37.0032	37.0391	37.0385	37.0017	35.5762	37.0027	36.3631
	8	42.5924	42.5407	42.5793	42.5912	42.4962	40.5814	42.5771	41.4359
	10	47.2110	47.1791	47.2474	47.3335	47.3048	45.1692	46.6687	45.1569
	12	51.6627	50.9570	51.0226	51.6421	51.0024	47.7623	51.6543	49.7426
9	4	30.2650	30.2650	30.2647	30.2650	30.2650	29.7961	30.2615	29.9921
	6	36.5929	36.5894	36.5848	36.5924	36.5903	34.7929	36.5877	35.9927
	8	42.0890	42.0789	42.0739	42.0757	42.0501	40.7925	42.0803	41.0783
	10	46.8554	46.7928	46.0774	46.8408	46.8110	44.5693	46.7586	45.2086
	12	51.1184	50.9838	50.9699	50.5265	51.0424	47.4544	50.9939	48.8786
10	4	32.3191	32.3127	32.3191	32.2953	32.3127	31.8869	32.3191	32.0323
	6	38.9318	38.8767	38.9250	38.9300	38.9223	37.9559	38.9258	38.3460
	8	44.6486	44.5368	44.6408	44.6440	44.4628	42.9020	44.6292	43.5905
	10	49.6640	49.5103	49.5058	49.6494	49.5299	47.0386	49.6353	48.4979
	12	54.1631	54.1038	54.0213	54.1207	54.0565	52.1343	54.0872	52.3326

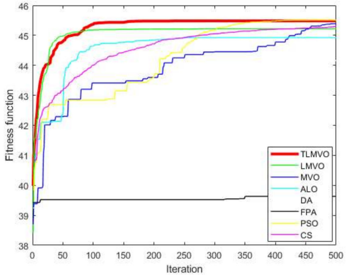

(a1) The values of Masi entropy under eight algorithms in Image 1

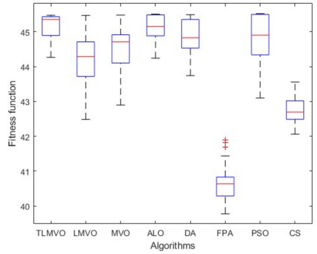

(a2) Box chart of fitness function values under eight algorithms in Image 1

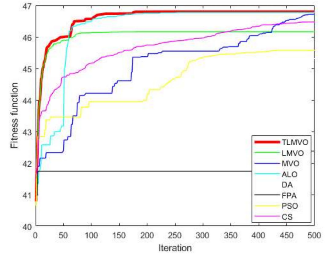

(b1) The values of Masi entropy under eight algorithms in Image 2

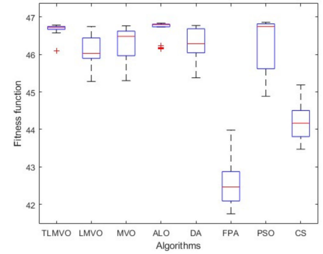

(b2) Box chart of fitness function values under eight algorithms in Image 2

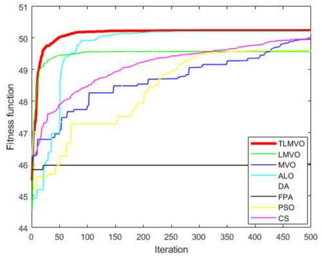

(c1) The values of Masi entropy under eight algorithms in Image 3

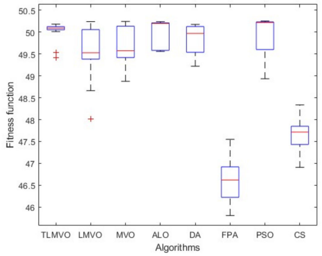

(c2) Box chart of fitness function values under eight algorithms in Image 3

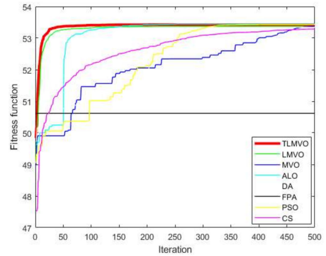

(d1) The values of Masi entropy under eight algorithms in Image 4

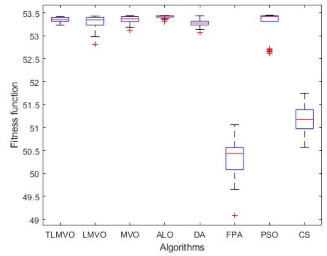

(d2) Box chart of fitness function values under eight algorithms in Image 4

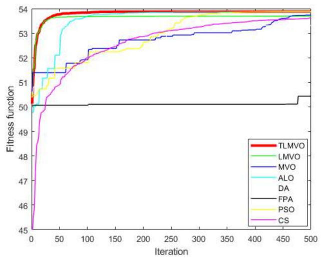

(e1) The values of Masi entropy under eight algorithms in Image 5

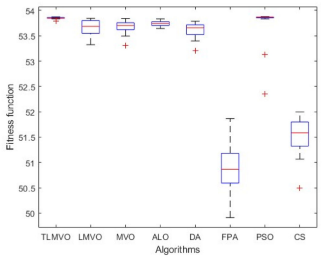

(e2) Box chart of fitness function values under eight algorithms in Image 5

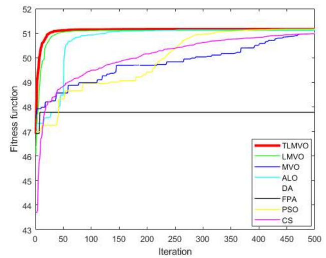

(f1) The values of Masi entropy under eight algorithms in Image 6

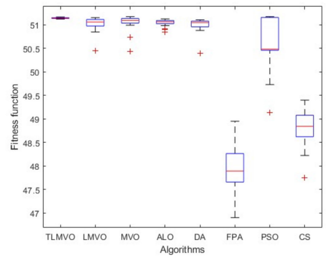

(f2) Box chart of fitness function values under eight algorithms in Image 6

Figure 10. *Cont.*

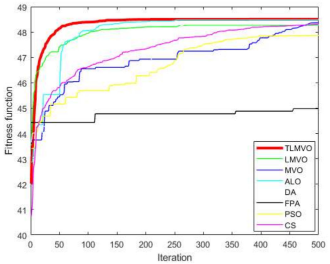

(g1) The values of Masi entropy under eight algorithms in Image 7

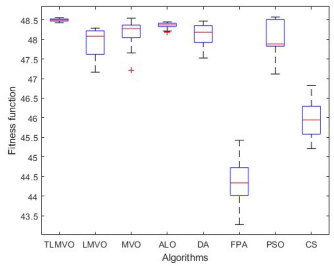

(g2) Box chart of fitness function values under eight algorithms in Image 7

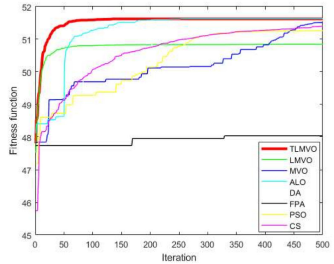

(h1) The values of Masi entropy under eight algorithms in Image 8

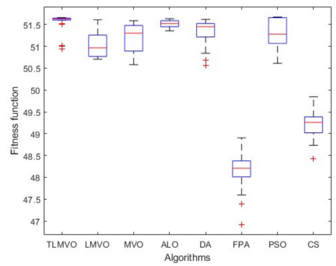

(h2) Box chart of fitness function values under eight algorithms in Image 6

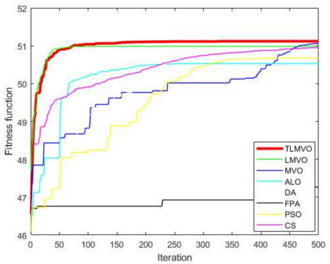

(i1) The values of Masi entropy under eight algorithms in Image 9

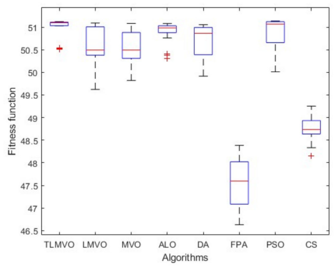

(i2) Box chart of fitness function values under eight algorithms in Image 9

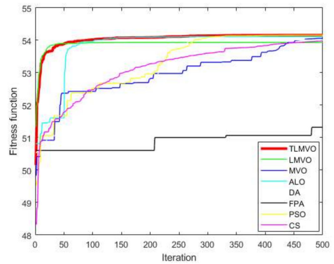

(j1) The values of Masi entropy under eight algorithms in Image 10

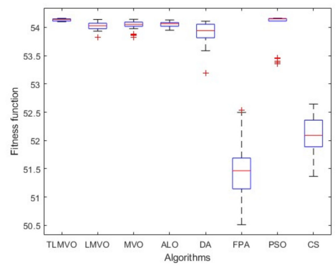

(j2) Box chart of fitness function values under eight algorithms in Image 10

Figure 10. The fitness function curves and box charts obtained by the TLMVO method of 10 satellite images.

As the fitness function of the application, a Masi entropy mathematical model is non-extensive and additive, which can provide better threshold results than other segmentation methods [23]. In the table of fitness function values, Table 8, it can be seen that PSO as a basic optimization algorithm can obtain better results at low thresholds. At high thresholds, the results of TLMVO, LMVO, MVO, ALO and DA have little difference. According to the label distribution, LMVO and ALO can be regarded as the second best. Figure 10 presents that:

1. In terms of convergence curve: in the early stage, TLMVO did not rapidly obtain a large value in the first 100 generations, as shown in Figure 10a1,b1,e1,i1,j1. In the 200th generation, TLMVO algorithm is faster than other algorithms to obtain the maximum target value or close to the theoretical maximum target value, as shown in Figure 10a1,b1,e1,g1,i1,j1. After the 250th generation, other algorithms are largely not updated.

However, for TLMVO, the advantages of ALO and CS position updating are used for reference, and mutation factors are added to maintain good population diversity and continuous updating in the later period of operation. As an improvement of the LMVO algorithm, TLMVO still retains the advantages of Lévy flight to avoid the algorithm falling into local optimization, and to be able to jump to a mutation space for optimization occasionally. On the basis of LMVO, the screening mechanism of the optimal solution is improved, and the mutation factor is added in the location update, which achieves better convergence and robustness. Traditional MVO population regeneration is slow and variation occurs at intervals. The convergence curve is stepped rather than a rising smooth curve. In addition to hybrid algorithms, ALO algorithm is always superior to other algorithms. The overall fluctuation of FPA algorithm is relatively large, while CS is relatively small. The optimal values found by them have large deviations, and some of them belong to local optimum values. Overall, TLMVO provides a competitive solution compared with other metaheuristics optimizers.

2. In terms of algorithm stability: In all box graphs, the TLMVO algorithm shows good stability, generally the best value and the second best value. For instance, the box plots in (b2) and (j2) are the second best values, and the rest are the best values, visually representing the stability of TLMVO. Other algorithms either float too much or have a lot of outliers.

In conclusion, compared with the comparison algorithm, TLMVO has higher optimization accuracy, better robustness and stability. The validity and superiority of the algorithm are proved, and the purpose of improving the basic LMVO and MVO algorithms is achieved.

5.4.3. Complexity Analysis

Algorithm complexity is another important indicator of performance. Complexity is related to population size, number of iterations, number of cycles, threshold size and other factors. The time complexity of TLMVO, LMVO and MVO can be expressed as $O(I * N * D) * O(F(x))$, where I represents the maximum number of iterations, N denotes the population size, D indicates the threshold value, and $F(x)$ corresponds to the Masi entropy function in this paper. As the number of thresholds increases, the complexity of the algorithm increases and the computing time becomes longer. In order to more intuitively analyze the computational complexity and time complexity of the algorithm, CPU time (in seconds) is selected for measurement. Each algorithm runs independently 30 times, and the average running time of the experiment is recorded in Table 9. The data in the table are integrated into a broken line graph, as shown in Figure 11. The image is used to sort the running time of each algorithm visually. The temporal ordering of algorithm can be expressed as (from large to small): $ALO > CS > DA > TLMVO > MVO > LMVO > PSO > FPA$. The results are in good agreement with the conclusions because the re-selected screening mechanism converges slowly. TLMVO is more effective for image segmentation when the time of TLMVO is similar to that of other algorithms.

Table 9. The the average CPU time of each algorithm under Masi.

TEST IMAGES	K	TLMVO	LMVO	MVO	ALO	DA	FPA	PSO	CS
1	4	0.4930	0.4260	0.4410	1.7600	0.7950	0.3790	0.4100	1.3240
	6	0.5100	0.4370	0.4640	2.3900	0.8090	0.3800	0.4120	1.3380
	8	0.5430	0.4640	0.4870	3.0440	0.8180	0.4110	0.4330	1.3460
	10	0.5700	0.4950	0.4990	3.7850	0.8200	0.4230	0.4520	1.3700
	12	0.6170	0.5230	0.5800	4.3320	0.8430	0.4520	0.4810	1.3860
2	4	0.6440	0.5330	0.6070	2.1550	1.0210	0.4990	0.5230	1.3950
	6	0.6650	0.5820	0.6130	2.9660	1.0430	0.5130	0.5520	1.4220
	8	0.7070	0.6030	0.6410	3.7150	1.0780	0.5460	0.5670	1.4390
	10	0.7550	0.6430	0.6840	4.6660	1.1390	0.5700	0.6070	1.4530
	12	0.7930	0.6770	0.7170	5.2850	1.1520	0.5980	0.6380	1.4920
3	4	0.6220	0.5820	0.6100	2.1440	0.9300	0.5020	0.5550	1.4400
	6	0.6970	0.6020	0.6360	2.9680	1.0870	0.5240	0.5690	1.4500
	8	0.7200	0.6360	0.6660	3.7530	1.0840	0.5700	0.5950	1.4610
	10	0.7650	0.6770	0.6970	4.6600	1.1190	0.5840	0.6350	1.4920
	12	0.7870	0.7300	0.7480	5.2680	1.1560	0.6050	0.6550	1.5000
4	4	0.6400	0.5820	0.6100	2.2110	1.0400	0.5080	0.5430	1.4210
	6	0.6910	0.6060	0.6440	3.0820	1.0830	0.5320	0.5710	1.4480
	8	0.7260	0.6310	0.6700	3.8380	1.1070	0.5680	0.6060	1.4640
	10	0.7650	0.6600	0.6930	4.7410	1.1380	0.5880	0.6250	1.4880
	12	0.8100	0.7010	0.7470	5.3380	1.1950	0.6230	0.6590	1.5140
5	4	0.6370	0.5680	0.6290	2.6220	1.0290	0.5450	0.5570	1.4130
	6	0.6930	0.5990	0.6450	2.9890	1.0950	0.5550	0.5700	1.4470
	8	0.7370	0.6260	0.6670	3.7710	1.1270	0.5660	0.5990	1.4500
	10	0.8100	0.6750	0.7180	4.7050	1.1650	0.5870	0.6270	1.4850
	12	0.8180	0.6900	0.7430	5.3290	1.1440	0.6080	0.6500	1.5030
6	4	0.6330	0.5740	0.5950	2.1830	0.9890	0.5340	0.5480	1.3790
	6	0.6900	0.5910	0.6450	2.9780	1.0840	0.5450	0.5590	1.4270
	8	0.7420	0.6510	0.6800	3.7890	1.1270	0.5660	0.5970	1.4570
	10	0.7470	0.6610	0.6960	4.7190	1.1920	0.6110	0.6150	1.4770
	12	0.8120	0.6880	0.7300	5.3230	1.2360	0.6040	0.6470	1.4960
7	4	0.6470	0.5808	0.6000	2.1550	1.0180	0.5030	0.5440	1.4140
	6	0.6670	0.5900	0.6290	3.0620	1.1050	0.5510	0.5840	1.4260
	8	0.7170	0.6530	0.6900	5.1410	1.2440	0.6050	0.6350	1.4920
	10	0.8270	0.7050	0.7550	5.4410	1.4680	0.6610	0.6770	1.6110
	12	0.9650	0.7880	0.7980	6.1020	1.3370	0.6390	0.6560	1.5610
8	4	0.7020	0.6280	0.6550	2.5230	1.1429	0.4980	0.5840	1.4040
	6	0.7360	0.6420	0.6730	3.5880	1.1470	0.5220	0.5910	1.4260
	8	0.7740	0.6540	0.6970	4.0550	1.1490	0.5480	0.6030	1.4440
	10	0.7890	0.6740	0.7460	5.2380	1.1510	0.5840	0.6230	1.4690
	12	0.8440	0.7200	0.7390	5.8670	1.2320	0.6270	0.6910	1.5100
9	4	0.7210	0.6390	0.6920	2.4750	1.0250	0.5920	0.6150	1.4800
	6	0.7860	0.6680	0.7560	3.3060	1.1820	0.5950	0.6330	1.5070
	8	0.8630	0.7210	0.7930	4.3700	1.3930	0.6080	0.6470	1.5110
	10	0.8900	0.7300	0.7660	5.5070	1.2570	0.6690	0.7070	1.5300
	12	0.9590	0.7690	0.8210	6.3310	1.4100	0.6870	0.7280	1.6470
10	4	0.6838	0.5580	0.6020	2.2140	1.0170	0.5180	0.5410	1.4290
	6	0.7070	0.5880	0.6400	3.0660	1.0700	0.5400	0.5790	1.4500
	8	0.7390	0.6250	0.6490	3.8670	1.1080	0.5900	0.6110	1.4710
	10	0.7790	0.6790	0.7050	4.8330	1.1280	0.6100	0.6390	1.4940
	12	0.8320	0.7110	0.7590	5.5270	1.1810	0.6320	0.6690	1.5140

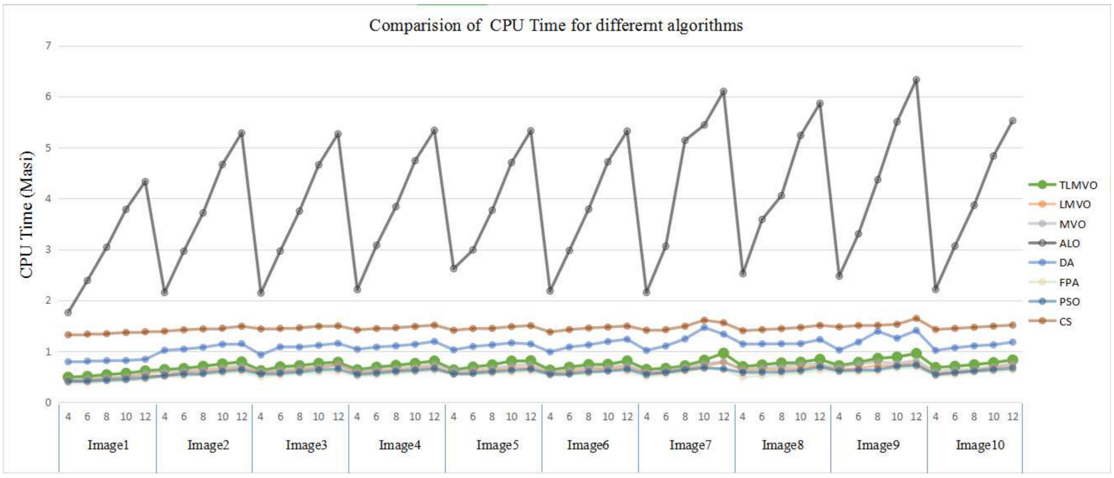

Figure 11. Broken line chart of the CPU Time indicator.

5.4.4. Statistical Analysis

In order to better analyze the results, we chose two more secure data statistical tests, namely Wilcoxon's rank sum test and Friedman test.

1. Wilcoxon's rank sum test is a pair-wise test, which aims to detect the significant difference between the mean values of two samples. In this paper, they correspond to the behavior of the two algorithms. The fitness function of GSMVO (K = 12) algorithm is compared with other seven algorithms. All algorithms run the same 30 times. The corresponding results are given in Table 10. The probability of a statistical value, the p-value and the indicator h are set throughout the test to determine whether to accept or reject the null hypothesis. Let the null hypothesis be: "There is no significant difference between the proposed algorithm and other algorithms." If the p-value is > 0.05 or h = 0, accept the null hypothesis, otherwise reject it. In addition, 67 of the 70 cases achieved superior results, which indicates that there is a significant difference between TLMVO and the other seven algorithms. In most cases, the TLMVO-based multilevel threshold algorithm outperforms the other seven algorithms.

Table 10. Average p-value of Wilcoxon test after 30 times of operation under Masi. (The data of $p > 0.05$ has been bolded, "+" indicates significant difference.).

TEST IMAGES	TLMVO vs. LMVO		TLMVO vs. MVO		TLMVO vs. ALO		TLMVO vs. DA		TLMVO vs. FPA		TLMVO vs. PSO		TLMVO vs. CS	
	p	**h**	***p***	**h**	***p***	**h**	***p***	**h**	***p***	**h**	***p***	**h**	***p***	**h**
1	<0.05+	1	<0.05	1	<0.05+	1	<0.05+	1	<0.05+	1	<0.05+	1	<0.05+	1
2	<0.05+	1	<0.05+	1	0.057	0	<0.05+	1	<0.05+	1	<0.05+	1	<0.05+	1
3	<0.05	1	<0.05	1	<0.05	1	<0.05+	1	<0.05+	1	<0.05	1	<0.05+	1
4	<0.05+	1	<0.05	1	<0.05+	1	<0.05+	1	<0.05+	1	<0.05+	1	<0.05+	1
5	<0.05+	1	<0.05	1	<0.05+	1	<0.05+	1	<0.05+	1	<0.05+	1	<0.05+	1
6	<0.05+	1	<0.05	1	<0.05	1	<0.05+	1	<0.05+	1	<0.05+	1	<0.05+	1
7	0.1952	0	<0.05	1	0.307	0	<0.05+	1	<0.05+	1	0.0072	1	<0.05+	1
8	<0.05+	1	<0.05	1	<0.05+	1	<0.05+	1	<0.05+	1	<0.05+	1	<0.05+	1
9	<0.05+	1	<0.05	1	<0.05	1	<0.05+	1	<0.05+	1	<0.05+	1	<0.05+	1
10	<0.05+	1	<0.05	1	<0.05	1	<0.05+	1	<0.05+	1	<0.05	1	<0.05+	1

2. Friedman test can be used to test the overall performance of data. The null hypothesis test approximate parameters are: H_0, the median of the equality between the algorithms; H_1, which is the alternative hypothesis, used to show the degree of difference; α: the rejection probability of the null hypothesis when the null hypothesis is true. If the p-value is less than the significance level, H_0 is rejected. A detailed description is in [67]. At one time, the rank serial numbers of the whole algorithm will be tested with the corresponding index data of the algorithm. It reflects the overall performance of

the algorithm intuitively and quickly. We put all the index data mentioned above into the test and get Table 11 (the highest ranking is marked with shadows). From the rankings obtained, TLMVO shows superiority in any threshold of different pictures, although sometimes the rankings are very close or the same.

After all experiments and results analysis, it can be concluded that TLMVO has greatly improved on LMVO and MVO. Compared with other metaheuristics algorithms, the TLMVO algorithm has better accuracy, convergence and robustness in multi-threshold color satellite image segmentation. This method can be used as an effective method for multilevel image threshold segmentation.

Table 11. The Friedman test of each algorithm under Masi.

TEST IMAGES	K	TLMVO	LMVO	MVO	ALO	DA	FPA	PSO	CS
1	4	1.8	3.2	4.2	5.3	3.8	6.4	4.1	7.2
	6	3	3.4	3.4	5	3.4	6.6	4.4	6.8
	8	2.8	3.6	4.2	3.2	5.2	6.6	3.4	7
	10	2.6	4.4	4	3	4	6	4.4	7.6
	12	1.8	2.6	4.6	3.6	4.8	6.6	5	7
2	4	2.4	3.6	4.2	4.6	4	5.2	6	6
	6	2.4	5.4	3.4	3.4	4	6.6	3.8	7
	8	2.8	3.4	4.4	3.2	5.2	6.4	3.4	7.2
	10	1.8	2.8	4	4.8	6	6.6	3	7
	12	1.8	4.2	4.6	3.4	3.4	6.6	5	7
3	4	2.6	4.4	3.8	5.4	3.2	6.6	4.2	5.8
	6	1.8	3.7	3.4	6	4.7	6.6	3.4	6.4
	8	2.8	3.4	4.8	3.6	4	6	3.8	7.6
	10	1.8	3.8	4.1	3.4	4.4	6.6	5.1	6.8
	12	1.8	4	4.4	4.6	5.4	6.6	2.2	7
4	4	2	3.2	3.4	5.5	4.4	6.6	4.3	6.6
	6	2.5	3.9	3.7	4.3	5.8	6.5	4	5.5
	8	1.9	2.9	3	4.4	6	6.6	4.2	7
	10	1	4.2	4.6	4	7	6.4	2.4	6.6
	12	1.8	3	3.4	5.4	6	5.4	3.6	7.4
5	4	2.8	4.2	5.9	4.4	6.4	4	3.2	5.1
	6	2.4	3	5.2	4.2	3.6	6	4	7.6
	8	1.5	3.3	3.4	5.6	5.6	6.6	3	7
	10	1.8	3	4	3.4	5.8	6	4.4	7.6
	12	2.8	3.8	4.8	4.2	3.2	6.6	3.6	7
6	4	1.8	3.4	3.6	4.4	6	6.6	3.2	7
	6	2.4	3.4	3.3	4.6	5.4	6.6	4.3	6
	8	1.8	4	4	4.4	3.4	6.6	4.8	7
	10	2.4	3.4	4.4	4.6	5.4	6.6	2.8	6.4
	12	2.4	2.9	4.8	3	5.4	6.6	3.9	7
7	4	2.6	3.8	4	3.8	6.2	5.6	4	6
	6	1.8	4.4	5.1	4.5	4.8	6.6	3.2	5.6
	8	2	3.8	5	3.4	5	6.6	3.2	7
	10	2.6	3.6	4.3	3.5	4.4	6.6	4	7
	12	1.8	3.2	4.4	3.6	5	6.6	4.4	7
8	4	1.8	3.3	4.8	3.6	5.5	5.4	4	7.6
	6	1.6	4.4	4.2	3	5.2	6.6	4	7
	8	1.8	3.8	4	4	5.8	6.6	3	7
	10	2.4	3.6	3.8	3.2	4.2	5.8	5.2	7.8
	12	1.8	3.8	4.2	4.8	5.8	6.6	2	7

Table 11. *Cont.*

TEST IMAGES	K	TLMVO	LMVO	MVO	ALO	DA	FPA	PSO	CS
9	**4**	2.1	2.4	4.2	5.4	5	6.4	3.3	7.2
	6	2.4	3.2	3	4.8	5.6	5.6	4.2	7.2
	8	2	2.7	3.5	4.6	6	6.6	3.6	7
	10	1.8	3.1	3.9	4.4	4.4	6	4.8	7.6
	12	1.8	3.8	4.2	5.8	3.6	6.4	3.2	7.2
10	**4**	3.4	3.6	4.5	5	3.8	5.2	4.1	6.4
	6	2.2	5.6	4.2	3	4.4	6.2	3.2	7.2
	8	2.4	2.4	3	4.9	6	6.2	3.7	7.4
	10	1.8	2.8	3.8	4.4	5.6	6.6	4	7
	12	1.8	2.8	3.4	4.4	5.8	6.4	4.2	7.2

6. Conclusions

This paper extensively studies the improved algorithm for color satellite image segmentation based on multilevel threshold. In order to solve the problem of a large amount of information and high precision of satellite image segmentation, a method combining the improved TLMVO algorithm with the much-anticipated Masi entropy in recent years is adopted. The results show that this method can be effectively applied to multilevel threshold segmentation of color images. Ten satellite images were used to test the multi-threshold performance of the algorithm. According to fitness function value, average CPU running time, Structural Similarity Index (SSIM), Feature Similarity Index (FSIM), and Peak Signal to Noise Ratio (PSNR), the segmentation results were evaluated. The results of Wilcoxon's rank sum test and Friedman test were analyzed. The validity and stability of the improved algorithm are verified by qualitative and quantitative methods. As an improvement of LMVO and MVO algorithms, Tournament selection mechanism that is more suitable for optimization algorithm was selected. Drawing on the merits of CS algorithm and ALO algorithm, the mutation factor is added to improve the position updating formula. Compared with other seven algorithms, TLMVO has better convergence and robustness. The multilevel threshold segmentation method based on TLMVO has broad application prospects. In future work, other new effective algorithms will be learned and improved, and a simpler and more efficient optimization method will be found. It is also applied to various computer vision problems such as satellite image enhancement, remote sensing image feature extraction and so on.

Author Contributions: X.P. contributed to the idea of this paper; X.P. and C.L. performed the experiments; X.P. wrote the paper; D.O. and H.J. contributed to the revision of this paper; Y.L. did the mapping; W.S. provided fund support.

Funding: This research was funded by the National Nature Science Foundation of China (No. 31470714).

Acknowledgments: The authors would like to thank the anonymous reviewers for their constructive comments and suggestions.

Conflicts of Interest: The authors declare no conflict of interest.

References

1. Wang, A.; Zhang, W.; Wei, X. A review on weed detection using ground-based machine vision and image processing techniques. *Comput. Electron. Agric.* **2019**, *158*, 226–240. [CrossRef]
2. Haindl, M.; Mikeš, S. A competition in unsupervised color image segmentation. *Pattern Recognit.* **2016**, *57*, 136–151. [CrossRef]
3. Ayala, H.V.H.; Santos, F.M.D.; Mariani, V.C. Image thresholding segmentation based on a novel beta differential evolution approach. *Expert Syst. Appl.* **2015**, *42*, 2136–2142. [CrossRef]
4. Bhandari, A.K.; Singh, V.K.; Kumar, A.; Singh, G.K. Cuckoo search algorithm and wind driven optimization based study of satellite image segmentation for multilevel thresholding using Kapur's entropy. *Expert Syst. Appl.* **2014**, *41*, 3538–3560. [CrossRef]

5. Mlakar, U.; Potočnik, B.; Brest, J. A hybrid differential evolution for optimal multilevel image thresholding. *Exp. Syst. Appl.* **2016**, *65*, 221–232. [CrossRef]
6. Gao, H.; Kwong, S.; Yang, J.; Cao, J. Particle swarm optimization based on intermediate disturbance strategy algorithm and its application in multi-threshold image segmentation. *Inf. Sci.* **2013**, *250*, 82–112. [CrossRef]
7. Bhandari, A.K.; Kumar, A.; Singh, G.K. Tsallis entropy based multilevel thresholding for colored satellite image segmentation using evolutionary algorithms. *Expert Syst. Appl.* **2015**, *42*, 8707–8730. [CrossRef]
8. Ali, M.; Ahn, C.W.; Pant, M. Multilevel image thresholding by synergetic differential evolution. *Appl. Soft Comput.* **2014**, *17*, 1–11. [CrossRef]
9. Mittal, H.; Saraswat, M. An optimum multilevel image thresholding segmentation using non-local means 2D histogram and exponential Kbest gravitational search algorithm. *Eng. Appl. Artif. Intell.* **2018**, *71*, 226–235. [CrossRef]
10. Sezgin, M. Survey over image thresholding techniques and quantitative performance evaluation. *J. Electron. Imaging* **2004**, *13*, 146–168.
11. Otsu, N. A threshold selection method from gray-level histograms. *IEEE Trans. Syst. Man Cybern.* **1979**, *9*, 62–66. [CrossRef]
12. Mohamed, H.; Merzban, M.E. Efficient solution of Otsu multilevel image thresholding: A comparative study. *Exp. Syst. Appl.* **2019**, *116*, 299–309.
13. Kapur, J.; Sahoo, P.K.; Wong, A.K. A new method forgray-level picture thresholding using the entropy of the histogram. *CVGIP* **1985**, *29*, 273–285.
14. Hinojosa, S.; Dhal, K.G.; Elaziz, M.A.; Oliva, D.; Cuevas, E. Entropy-based imagery segmentation for breast histology using the Stochastic Fractal Search. *Neurocomputing* **2018**, *321*, 201–215. [CrossRef]
15. Pal, S.K.; King, R.A.; Hashim, A.A. Automatic gray level thresholding through index of fuzziness and entropy. *Pattern Recognit. Lett.* **1983**, *1*, 141–146. [CrossRef]
16. Sarkar, S. A differential evolutionary multilevel segmentation of near infra-red images using Renyi's entropy. In Proceedings of the International Conference on Frontiers of Intelligent Computing: Theory and Applications (FICTA); Springer: Berlin/Heidelberg, Germany, 2013; Volume 199, pp. 699–706.
17. Shannon, C.E. A mathematical theory of communication. *MD Comput.* **1997**, *14*, 306–317. [PubMed]
18. Albuquerque, M.P.D.; Esquef, I.A.; Mello, A.R.G. Image thresholding using Tsallis entropy. *Pattern Recognit. Lett.* **2004**, *25*, 1059–1065. [CrossRef]
19. Sumathi, R.; Venkatesulu, M.; Arjunan, S.P. Extracting tumor in MR brain and breast image with Kapur's entropy based Cuckoo Search Optimization and morphological reconstruction filters. *Biocybern. Biomed. Eng.* **2018**, *38*, 918–930. [CrossRef]
20. Lopez-Garcia, P.; Onieva, E.; Osaba, E. A metaheuristics based in the hybridization of Genetic Algorithms and Cross Entropy methods for continuous optimization. *Expert Syst. Appl.* **2016**, *55*, 508–519. [CrossRef]
21. Pare, S.; Bhandari, A.K.; Kumar, A.; Singh, G.K. A new technique for multilevel color image thresholding based on modified fuzzy entropy and Lévy flight firefly algorithm. *Comput. Electr. Eng.* **2017**, *70*, 476–495. [CrossRef]
22. Naidu, M.S.R.; Rajesh Kumar, P.; Chiranjeevi, K. Shannon and Fuzzy entropy based evolutionary image thresholding for image segmentation. *Alex. Eng. J.* **2017**, *57*, 1643–1655. [CrossRef]
23. Masi, M. A step beyond Tsallis and Rényi entropies. *Phys. Lett.* **2005**, *338*, 217–224. [CrossRef]
24. Kandhway, P.; Bhandari, A.K. A Water Cycle Algorithm-Based Multilevel Thresholding System for Color Image Segmentation Using Masi Entropy. *Circuits Syst. Signal Process.* **2018**, 1–49. [CrossRef]
25. Shubham, S.; Bhandari, A.K. A generalized Masi entropy based efficient multilevel thresholding method for color image segmentation. *Multimed. Tools Appl.* **2019**, 1–42. [CrossRef]
26. Wolpert, D.H.; Macready, W.G. No free lunch theorems for optimization. *Trans. Evol. Comput.* **1997**, *1*, 67–82. [CrossRef]
27. Talbi, E.G. A taxonomy of hybrid metaheuristics. *J. Heuristics* **2002**, *8*, 541–564. [CrossRef]
28. Baniani, E.A.; Chalechale, A. Hybrid PSO and genetic algorithm for multilevel maximum entropy criterion threshold selection. *Int. J. Hybrid Inf. Technol.* **2013**, *6*, 131–140. [CrossRef]
29. Mafarja, M.M.; Mirjalili, S. Hybrid Whale Optimization Algorithm with simulated annealing for feature selection. *Neurocomputing* **2017**, *260*, 302–312. [CrossRef]
30. Mirjalili, S.; Mirjalili, S.M. A Hatamlou, Multiverse Optimizer: A nature-inspired algorithm for global optimization. *Neural Comput. Appl.* **2016**, *27*, 495–513. [CrossRef]

31. Ali, E.E.; El-Hameed, M.A.; El-Fergany, A.A.; El-Arini, M.M. Parameter extraction of photovoltaic generating units using multi-verse optimizer. *Sustain. Energy Technol. Assess.* **2016**, *17*, 68–76. [CrossRef]
32. Jangir, P.; Parmar, S.A.; Trivedi, I.N.; Bhesdadiya, R.H. A novel hybrid Particle Swarm Optimizer with multi verse optimizer for global numerical optimization and Optimal Reactive Power Dispatch problem. *Eng. Sci. Technol. Int. J.* **2017**, *20*, 570–586. [CrossRef]
33. Wang, X.; Luo, D.; Zhao, X.; Sun, Z. Estimates of energy consumption in China using a self-adaptive multi-verse optimizer-based support vector machine with rolling cross-validation. *Energy* **2018**, *152*, 539–548. [CrossRef]
34. Elaziz, M.A.; Oliva, D.; Ewees, A.A.; Xiong, S. Multilevel thresholding-based grey scale image segmentation using multi-objective multi-verse optimizer. *Expert Syst. Appl.* **2019**, *125*, 112–129. [CrossRef]
35. Noraini, M.; Geraghty, J. Genetic algorithm performance with different selection strategies in solving TSP. *World Congr. Eng.* **2011**, *II*, 4–9.
36. Medhane, D.V.; Sangaiah, A.K. Search space-based multi-objective optimization evolutionary algorithm. *Comput. Electr. Eng.* **2017**, *58*, 126–143.
37. Jia, H.; Peng, X.; Song, W.; Lang, C.; Xing, Z.; Sun, K. Multiverse Optimization Algorithm Based on Lévy Flight Improvement for Multithreshold Color Image Segmentation. *IEEE Access* **2019**, *7*, 32805–32844. [CrossRef]
38. Barrow, J.D.; Davies, P.C.W.; Harper, C.L. Science and Ultimate Reality: Quantum Theory, Cosmology and Complexity. *Am. J. Phys.* **2004**, *74*, 245–247.
39. Khoury, J.; Ovrut, B.A.; Seiberg, N.; Steinhardt, P.J.; Turok, A.N. From big crunch to big bang. *Phys. Rev. D* **2001**, *65*, 381–399. [CrossRef]
40. Yang, X.S.; Deb, S. Cuckoo Search via Lévy Flights. *Mathematics* **2010**, *71*, 210–214.
41. Joshi, A.S.; Kulkarni, O. Cuckoo search optimization—A review. *Sci. Direct Mater.* **2017**, *4*, 7262–7269. [CrossRef]
42. Yang, X.S. Flower pollination algorithm for global optimization. *Unconv. Comput. Nat. Comput.* **2012**, *7445*, 240–249.
43. Shen, L.; Fan, C.; Huang, X. Multilevel image thresholding using modified flower pollination algorithm. *IEEE Access* **2018**, *6*, 30508–30518. [CrossRef]
44. Xu, L.; Jia, H.; Lang, C.; Peng, X.; Sun, K. A novel method for multilevel color image segmentation based on dragonfly algorithm and differential evolution. *IEEE Access* **2019**, *99*, 2169–3536. [CrossRef]
45. Goldberg, D.E.; Deb, K. A comparative analysis of selection schemes used in genetic algorithms. *Found. Genet. Algorithms* **1991**, *1*, 69–93.
46. *Handbook of Evolutionary Computation*; IOP Publishing Ltd.: Bristol, UK; Oxford University Press: Oxford, UK, 1997.
47. Blickle, T.; Thiele, L. A Comparison of Selection Schemes used in Genetic Algorithms. *Evol. Comput.* **1996**, *4*, 361–394. [CrossRef]
48. Baker, J.E. Adaptive Selection Methods for Genetic Algorithms. In Proceedings of the First International Conference on Genetic Algorithms & Their Applications, Pittsburg, CA, USA, 24–26 July 1985.
49. Li, J.; Tan, Y. Loser-Out Tournament-Based Fireworks Algorithm for Multimodal Function Optimization. *IEEE Trans. Evol. Comput.* **2017**, *99*. [CrossRef]
50. Das, S.; Mallipeddi, R.; Maity, D. Adaptive evolutionary programming with p-best mutation strategy(Article). *Swarm Evol. Comput.* **2013**, *9*, 58–68. [CrossRef]
51. Al-Betar, M.A.; Awadallah, M.A.; Khader, A.T.; Bolaji, A.L. Tournament-based harmony search algorithm for non-convex economic load dispatch problem. *Appl. Soft Comput.* **2016**, *47*, 449–459. [CrossRef]
52. Ralf, M.; Klafter, J. The random walk's guide to anomalous diffusion: A fractional dynamics approach. *Phys. Rep.* **2000**, *339*, 1–77.
53. Dinkar, S.K.; Deep, K. An efficient opposition based Lévy Flight Antlion optimizer for optimization problems. *Int. J. Comput. Sci.* **2018**, *29*, 119–141. [CrossRef]
54. Zhang, H.; Xie, J.; Hu, Q.; Shao, L.; Chen, T. A hybrid DPSO with Lévy flight for scheduling MIMO radar tasks. *Appl. Soft Comput.* **2018**, *71*, 242–254. [CrossRef]
55. Jain, M.; Singh, V.; Rani, A. A novel nature-inspired algorithm for optimization: Squirrel search algorithm. *Swarm Evol. Comput.* **2019**, *44*, 148–175. [CrossRef]
56. Mirjalili, S. The Ant Lion Optimizer. *Adv. Eng. Softw.* **2015**, *83*, 80–98. [CrossRef]

57. Kennedy, J. Particle swarm optimization. In Proceedings of the ICNN'95 International Conference on Neural Networks, Perth, WA, Australia, 27 November–1 December 1995; Volume 4, pp. 1942–1948.
58. Akay, B. A study on particle swarm optimization and artificial bee colony algorithms for multilevel thresholding. *Appl. Soft Comput.* **2013**, *13*, 3066–3091. [CrossRef]
59. Liu, Y.; Mu, C.; Kou, W.; Liu, J. Modified particle swarm optimization-based multilevel thresholding for image segmentation. *Soft Comput.* **2015**, *19*, 1311–1327. [CrossRef]
60. Gao, H.; Pun, C.M.; Kwong, S. An efficient image segmentation method based on a hybrid particle swarm algorithm with learning strategy. *Inf. Sci.* **2016**, *369*, 500–521. [CrossRef]
61. Wang, M.; Wu, C.; Wang, L.; Xiang, D.; Huang, X. A feature selection approach for hyperspectral image based on modified ant lion optimizer. *Knowl. Based Syst.* **2019**, *168*, 39–48. [CrossRef]
62. The Aerial Data Set. Available online: https://landsat.visibleearth.nasa.gov/view.php?id=144523 (accessed on 10 March 2019).
63. Pare, S.; Kumar, A.; Bajaj, V.; Singh, G.K. An efficient method for multilevel color image thresholding using cuckoo search algorithm based on minimum cross entropy. *Appl. Soft Comput.* **2017**, *61*, 570–592. [CrossRef]
64. Wang, Z.; Bovik, A.C.; Sheikh, H.R.; Simoncelli, E.P. Image quality assessment: From error visibility to structural similarity. *IEEE Trans. Image Process.* **2004**, *13*, 600–612. [CrossRef]
65. Zhang, L.; Zhang, L.; Mou, X. FSIM: A Feature Similarity Index for Image Quality Assessment. *IEEE Trans. Image Process.* **2011**, *20*, 2378–2386. [CrossRef]
66. Roy, R.; Laha, S. Optimization of stego image retaining secret information using genetic algorithm with 8-connected PSNR. *Procedia Comput. Sci.* **2015**, *60*, 468–477. [CrossRef]
67. Pare, S.; Bhandari, A.K.; Kumar, A.; Singh, G.K. An optimal color image multilevel thresholding technique using grey-level co-occurrence matrix. *Expert Syst. Appl.* **2017**, *87*, 335–362. [CrossRef]
68. Oliva, D.; Hinojosa, S.; Cuevas, E.; Pajares, G.; Avalos, O.; Gálvez, J. Cross entropy based thresholding for magnetic resonance brain images using Crow Search Algorithm. *Expert Syst. Appl.* **2017**, *79*, 164–180. [CrossRef]
69. Ibrahim, R.A.; Elaziz, M.A.; Lu, S. Chaotic opposition-based grey-wolf optimization algorithm based on differential evolution and disruption operator for global optimization. *Expert Syst. Appl.* **2018**, *108*, 1–27. [CrossRef]
70. Derrac, J.; García, S.; Molina, D.; Herrera, F. A practical tutorial on the use of nonparametric statistical tests as a methodology for comparing evolutionary and swarm intelligence algorithms. *Swarm Evol. Comput.* **2011**, *1*, 3–18. [CrossRef]